Remote Sensing of Environment 187 (2016) 345–366

Contents lists available at ScienceDirect

Remote Sensing of Environment

journal homepage: www.elsevier.com/locate/rse

Photosynthetic efficiency of northern forest ecosystems using a MODIS-derived Photochemical Reflectance Index (PRI)

E.M. Middleton [a], K.F. Huemmrich [b], D.R. Landis [c,*], T.A. Black [d], A.G. Barr [e], J.H. McCaughey [f]

[a] Biospheric Sciences Laboratory, NASA/Goddard Space Flight Center, Greenbelt, MD 20771, USA
[b] Joint Center for Earth Tech., University of Maryland at Baltimore County, Baltimore, MD 21228, USA
[c] Global Science & Technology, Inc., Greenbelt, MD 20770, USA
[d] University of British Columbia, Vancouver, British Columbia, Canada
[e] Climate Research Branch, Meteorological Service of Canada, Saskatoon, Saskatchewan, Canada
[f] Queens University, Kingston, Ontario, Canada

ARTICLE INFO

Article history:
Received 1 April 2016
Received in revised form 19 September 2016
Accepted 10 October 2016
Available online 31 October 2016

Keywords:
Light use efficiency, LUE
MODIS
MODIS GPP
PRI
Terra, Aqua
Canadian Carbon Program
Boreal forests
Forward scatter

ABSTRACT

This study evaluates a direct remote sensing approach from space for the determination of ecosystem photosynthetic light use efficiency (LUE), through measurement of vegetation reflectance changes expressed with the Photochemical Reflectance Index (PRI). The PRI is a normalized difference index based on spectral changes at a physiologically active wavelength (~531 nm) as compared to a reference waveband, and is only available from a very few satellites. These include the two Moderate-Resolution Imaging Spectroradiometers (MODIS) on the Aqua and Terra satellites each of which have a narrow (10 nm) ocean band centered at 531 nm. We examined several PRI variations computed with candidate reference bands, since MODIS lacks the traditional 570 nm reference band. The PRI computed using MODIS land band 1 (620–670 nm) gave the best performance for daily LUE estimation. Through rigorous statistical analyses over a large image collection ($n = 420$), the success of relating in situ daily tower-derived LUE to MODIS observations for northern forests was strongly influenced by satellite viewing geometry. LUE was calculated from CO_2 fluxes (mol C mol^{-1} absorbed quanta) measured at instrumented Canadian Carbon Program flux towers in four Canadian forests: a mature fir site in British Columbia, mature aspen and black spruce sites in Saskatchewan, and a mixed deciduous/coniferous forest site in Ontario. All aspects of the viewing geometry had significant effects on the MODIS-PRI, including the view zenith angle (VZA), the view azimuth angle, and the displacement of the view azimuth relative to the solar principal plane, in addition to illumination related variables. Nevertheless, we show that forward scatter sector views (VZA, 16°–45°) provided the strongest relationships to daily LUE, especially those collected in the early afternoon by Aqua ($r^2 = 0.83$, RMSE = 0.003 mol C mol^{-1} absorbed quanta). Nadir (VZA, 0° ± 15°) and backscatter views (VZA, −16° to −45°) had lower performance in estimating LUE (nadir: r^2 ~ 0.62–0.67; backscatter: r^2 ~ 0.54–0.59) and similar estimation error (RMSE = 0.004–0.005). When directional effects were not considered, only a moderately successful MODIS-PRI vs. LUE relationship ($r^2 = 0.34$, RMSE = 0.007) was obtained in the full dataset (all views & sites, both satellites), but site-specific relationships were able to discriminate between coniferous and deciduous forests. Overall, MODIS-PRI values from Terra (late morning) were higher than those from Aqua (early afternoon), before/after the onset of diurnal stress responses expressed spectrally. Therefore, we identified ninety-two Terra-Aqua "same day" pairs, for which the sum of Terra morning and Aqua afternoon MODIS-PRI values (PRI_{sum}) using all available directional observations was linearly correlated with daily tower LUE ($r^2 = 0.622$, RMSE = 0.013) and independent of site differences or meteorological information. Our study highlights the value of off-nadir directional reflectance observations, and the value of pairing morning and afternoon satellite observations to monitor stress responses that inhibit carbon uptake in Canadian forest ecosystems. In addition, we show that MODIS-PRI values, when derived from either: (i) forward views only, or (ii) Terra/Aqua same day (any view) combined observations, provided more accurate estimates of tower-measured daily LUE than those derived from either nadir or backscatter views or those calculated by the widely used semi-operational MODIS GPP model (MOD17) which is based on a theoretical maximum LUE and environmental data. Consequently, we demonstrate the importance of diurnal as well as off-nadir satellite observations for detecting vegetation physiological processes.

* Corresponding author.
E-mail addresses: elizabeth.m.middleton@nasa.gov (E.M. Middleton), david.r.landis@nasa.gov (D.R. Landis).

http://dx.doi.org/10.1016/j.rse.2016.10.021
0034-4257/

1. Introduction

Mapping the dynamics of terrestrial carbon exchange and understanding its response to climate changes are high priorities for Earth System research (e.g., Margolis et al., 2006; Michalak et al., 2011). A satellite measurement approach based on direct observations would greatly simplify and amplify our ability to track surface/atmosphere carbon exchange processes. However, regional studies currently rely on ecosystem models that require extensive environmental and/or meteorological information or simple assumptions to compute regional source and sink strengths (e.g., Baker et al., 2008; Kucharik and Twine, 2007; Potter et al., 1993; Thornton et al., 2005; Weng and Luo, 2008). A commonly employed modeling approach relies on describing down-regulation of the assumed optimal performance in carbon uptake due to environmental stresses (e.g., nutrient, moisture, or vapor pressure deficits, and temperature extremes). Not only is this down-regulation difficult to model, but some model inputs, such as root zone soil moisture, are not available at the necessary spatial scales.

1.1. Modeling LUE

One widely adopted modeling approach for ecosystem carbon uptake is the light use efficiency (LUE) concept. This type of model determines vegetation production as a linear function of absorbed photosynthetically active radiation (APAR), with the basic form:

$$G = \varepsilon \, fAPAR \, Q_{in} \tag{1}$$

where G is gross primary production (GPP), Q_{in} is the incident photosynthetically active radiation (PAR), fAPAR is the fraction of PAR absorbed by green vegetation, and ε is the LUE, a measure of the plant's ability to convert this absorbed energy into biomass (Monteith, 1977; Russell et al., 1989; Garbulsky et al., 2011). Though originally formulated to quantify the biomass accumulation as a function of available PAR over a growing season in crops, this simple concept has been adapted for estimating shorter term (e.g., hourly, daily, weekly, monthly) carbon uptake by ecosystems, especially at flux tower sites (e.g., Turner et al., 2003). However, the critical factor in the LUE model describing ecosystem physiological function, ε, varies with plant type, age, pigment levels, and environmental conditions over space and time. These environmental factors (e.g., temperature, soil type, water availability, humidity, disease, and nutrient availability) are needed to parameterize ecosystem models of surface/atmosphere carbon exchange (Prince, 1991; Gamon et al., 2001). Critical environmental variables also include soil water deficits, low temperatures, and atmospheric vapor pressure deficits (e.g., Landsberg, 1986; Law and Waring, 1994; Runyon et al., 1994; Prince and Goward, 1995). Typically, most of this information is lacking.

For this reason, the essential ε term in the LUE model (Eq. 1) has been estimated in different ways and incorporated along with remotely sensed data into various LUE models to determine carbon fluxes (e.g., Jenkins et al., 2007; Yuan et al., 2007; Yuan et al., 2014; Alton, 2016). Some widely used LUE models are based on an assumed maximum unstressed light use efficiency (ε^*) for a given vegetation type. In that approach, modifying functions scaled between 0 and 1 are coupled with critical environmental variables to reduce ε^* in an attempt to achieve a more realistic estimate of the actual value of ε. The gross primary production (GPP) product from the Moderate-Resolution Imaging Spectroradiometer (MODIS) satellite data (MOD17) uses a version of this approach, by adjusting ε^* for each pixel's broad category vegetation type (e.g., deciduous forest, coniferous forest, grassland) to estimate LUE based on daily minimum temperature and daytime average vapor pressure deficit (Heinsch et al., 2003; Running et al., 2004).

1.2. The Photochemical Reflectance Index

An alternative approach to estimate LUE with less dependency on explicit meteorological information is based on direct spectral observations, and has successfully been demonstrated with in situ measurements at leaf, above-canopy, and flux tower local scales. This alternative remote sensing approach is based on direct detection with the Photochemical Reflectance Index (PRI) of vegetation responses to physiologically stressful conditions that produce a down-regulation of photosynthesis over short (e.g., diurnal) time periods (e.g., Gamon et al., 1992, 1997; Magney et al., 2016).

The PRI is an indicator of the relative expression of a daily protective biochemical cycle involving xanthophyll pigments, which are specific types of carotenoid photosynthetic pigments, in response to high irradiance or related conditions (e.g., high temperatures, water deficit, low stroma pH; refer to Middleton et al., 2009a, 2012). Typically, this reversible, protective mechanism is most strongly expressed from mid-day through mid-afternoon when these physiological stresses are most limiting to photosynthetic function (e.g., Zarco-Tejada et al., 2012, 2013a, 2013b), thus causing what is referred to as "down regulation" of photosynthesis. In circumstances when a leaf's PAR absorption exceeds the capacity of its photosynthetic processes to use that energy, especially under high illumination and water deficits, reactions in the xanthophyll cycle cause the pigment violaxanthin to form zeaxanthin via antheraxanthin, a process referred to as de-epoxidation. This process releases energy as heat and is reversible when PAR levels are reduced (Müller et al., 2001). These photochemical changes by xanthophyll pigments cause an observable change in leaf reflectance at 531 nm (e.g., Gamon et al., 1992; Peñuelas et al., 1995; Atherton et al., 2016).

The PRI is a spectral index based on two narrow (≤10 nm) visible bands, one of which centers on the physiologically active wavelength at 531 nm, combined in a normalized difference ratio with a reference wavelength (Gamon et al., 1992, 1997; Gamon and Qiu, 1999; Filella et al., 1996; Grace et al., 2007; Garbulsky et al., 2011; Middleton et al., 2009a, 2009b, 2012), and is unitless. This is typically expressed as:

$$PRI = (\rho_{531} - \rho_{ref})/(\rho_{531} + \rho_{ref}) \tag{2}$$

where ρ_{531} is the reflectance at 531 nm, the center wavelength of the spectral region most sensitive to the epoxidation state of the xanthophyll cycle pigments, and ρ_{ref} is a second unaffected band that serves as a reference. Different wavelength bands have been used for ρ_{ref} (e.g., Drolet et al., 2008; Middleton et al., 2009a; Goerner et al., 2009) but the originally suggested 570 nm band is used most often (Gamon et al., 1992, 1997). While the PRI spectral index is specifically designed to detect this reaction in facultative (daily) cycles, it can be influenced by conformational changes in chloroplasts and changes in stroma pH (Filella et al., 2009; Gamon and Berry, 2012), as well as by longer term (constitutive) seasonal changes in foliage chlorophyll:carotenoid pigment ratios (Stylinski et al., 2002; Filella et al., 2009; Garrity et al., 2011; Wong and Gamon, 2015a, 2015b; Gamon and Berry, 2012; Magney et al., 2016; Gamon et al., 2016).

At the canopy level, the PRI has been shown to exhibit anisotropy, varying along the illuminated path of the sun – referred to as the solar principle plane (SPP) – as a function of viewing geometry, especially the view zenith angle (VZA), in coniferous forests and cornfields (e.g., Nichol et al., 2000; Cheng et al., 2009, 2010; Middleton et al., 2009a, 2009b, 2014, 2015), as a component of the bidirectional reflectance function (BRDF). In particular, the PRI has been shown to exhibit higher values along the SPP in the canopy cold spot (or dark spot) associated with forward scattered reflectance (viewed facing towards the sun) and lower values at nadir or in the hotspot (or bright spot) associated with backscattered reflectance (viewed facing directly away from the sun) (Cheng et al., 2009, 2010; Middleton et al., 2009a, 2009b, 2014, 2015; Hilker et al., 2008, 2009; Hall et al., 2008). The cold spot/dark spot and hotspot/bright spot are often linked to shaded vs. sunlit

canopy sectors, respectively (e.g., Middleton et al., 2009a). The anisotropy associated with the PRI can be affected by the relative amount of direct and diffuse shortwave illumination (Damm et al., 2015).

The PRI is known to be an important indicator of variations in photosynthetic efficiency rates (Gamon et al., 1992; Peñuelas et al., 1995), and the relationship between PRI and LUE has been established for a number of different species (Gamon et al., 1997; Peñuelas et al., 1995) at both the leaf and canopy level (Gamon et al., 1992; Filella et al., 1996; Nichol et al., 2000; Rahman et al., 2001; Raddi et al., 2001; Hilker et al., 2008; Strachan et al., 2008; Middleton et al., 2009b, 2014; Peñuelas et al., 2011). The PRI behavior was examined over full growing seasons in two forests in conjunction with flux towers, indicating methods to improve the relationship to LUE but noting the influence of confounding factors (Soudani et al., 2014). A recent study of a tropical evergreen forest found that PRI combined with vapor pressure deficit information performed reasonably well for LUE (Nakaji et al., 2016). A number of review papers on PRI and its use in determining carbon fluxes have been published over the past few years, indicating the maturing of this field (Grace et al., 2007; Hilker et al., 2008; Coops et al., 2010; Garbulsky et al., 2011; Peñuelas et al., 2011; Middleton et al., 2012).

The conventional PRI (using wavelengths at 531 and 570 nm) produces a range of values that can be interpreted in terms of degree of expressed physiological stress, where negative values, especially those below −0.2, indicate that stress is pronounced, whereas positive values indicate only small (or no) stress effects, and those above +0.2 indicate near optimal photosynthetic function (Middleton et al., 2014, Middleton et al., 2015, Cheng et al., 2013). However, the interpretation of vegetation stress/photosynthetic function associated with the range of values computed with other PRI variations (using reference bands other than 570 nm) has not been addressed.

1.3. PRI from satellites

Currently, there are very few options to acquire the PRI from satellite remote sensing platforms. One of the few possible options uses hyperspectral data from the Hyperion imaging spectrometer on NASA's Earth Observing One (EO-1) satellite, which enables the use of the conventional PRI (Asner et al., 2004; Campbell et al., 2013; Huemmrich et al., 2013; Zhang et al., 2016) at a relatively high spatial resolution (30 m) for user-selected sites. The PRI has also been studied using imagery acquired from the European Space Agency's (ESA's) Proba-1 satellite's primary instrument, the Compact High Resolution Imaging Spectrometer, referred to as CHRIS PROBA, which has a nadir ground resolution of 17 m and observes four additional view angles (±36°, ±55°) in 18 user-selected visible through near-infrared (VNIR) narrow spectral bands (Raddi et al., 2006; Hilker et al., 2011; Stagakis et al., 2014). Most other satellite studies have used NASA's operational MODIS Terra and Aqua sensors because they have the critical narrow green band (ocean Band 11, 526–536 nm), and provide frequent global coverage.

MODIS's green ocean Band 11, necessary for calculation of PRI, is one of the coarse spatial resolution (1-km) ocean bands that are generally not used over land. While the Terra and Aqua orbits and MODIS spectral bands were neither optimized nor even envisioned for this particular terrestrial ecosystem application, several studies have nevertheless shown relationships between a MODIS-derived PRI and in situ LUE of forests determined from carbon flux data measured at instrumented towers using eddy covariance methods (e.g., Rahman et al., 2004; Drolet et al., 2005, 2008; Goerner et al., 2011; Sims et al., 2011; Guarini et al., 2014). For example, the Goerner et al. (2011) study examined five widely distributed mid-latitude sites to include savanna and multiple forest types (evergreen broadleaf, needle-leaved, and deciduous broadleaf forests) and found site-dependent relationships between MODIS-PRI and in situ LUE that were as good or better than approaches using meteorological variables.

Most of these MODIS-PRI studies for LUE estimation have used the two green ocean bands – 11 (for xanthophyll responses) and 12 (546–556 nm as reference) – and they have incorporated data acquired with different ranges of off-nadir and/or nadir viewing geometries from either (or both) Terra and Aqua (Rahman et al., 2004; Drolet et al., 2005; Drolet et al., 2008; Sims et al., 2011; Guarini et al., 2014). In both Rahman et al. (2004) and Drolet et al. (2005), relationships between MODIS-PRI and LUE were developed for only a single site from Terra observations. Guarini et al. (2014) studied Mediterranean oak forests over two years, also finding moderate correlations between MODIS-PRI from Terra for backscattered observations during a wet (low stress) year. However, viewing geometry did not significantly affect this MODIS-PRI from a study when both Terra and Aqua were used throughout the growing season in three mid-latitude deciduous forested sites (Sims et al., 2011). Drolet et al. (2008) examined multiple boreal conifer sites that represented a chronosequence dominated by the same species; using relationships developed between MODIS-PRI from backscatter observations and LUE from these sites, from which a LUE map for a 5300 km^2 region in Saskatchewan was produced. This accomplishment revealed local LUE variability at the scale of a few kilometers, a capability that presently cannot be achieved using approaches driven by coarse-scale regional meteorological data.

When MODIS-PRI was computed at a mid-latitude Mediterranean oak site (Goerner et al., 2009) using one of the MODIS red spectral bands as the reference band, improved associations with tower LUE were obtained. The use of this red land band (Band 1, 50 nm wide, centered at 645 nm, 250-m spatial resolution at nadir) provided stronger results than use of a narrow red ocean band (Band 13, 10 nm wide, centered at 667 nm) having coarser spatial resolution (1-km).

In addition to differences due to the choice of reference spectral band, differences in the PRI performances across studies can be attributed to observation geometry differences among sites and dates. The influence of viewing geometry on MODIS-PRI is not unexpected since canopy PRI anisotropy has already been noted. Similarly, directional influences have been reported for MODIS vegetation indices, including the Normalized Difference Vegetation Index (NDVI), for which higher NDVI values in the forward scatter view sectors were reported for MODIS data (Huete et al., 2002; Fensholt et al., 2010) and by earlier polar orbiting wide swath environmental satellites (Holben, 1986; van Leeuwen et al., 1999). Early methods to produce MODIS temporal composites from individual scenes preferentially included imagery with higher NDVI values per pixel, as a shortcut to evaluating which were collected under clear-sky conditions, until it was recognized that these higher values were often acquired in the forward scatter views, such that their predominance biased the computed average nadir response (Fensholt et al., 2010). Therefore, a decision was made early in the Terra mission to standardize surface reflectance to nadir views for temporal composites. While this approach has minimized the day to day variations for nadir views acquired with MODIS sensors, the independent study of dynamic vegetation properties with non-nadir views has not been actively pursued nor has the potential for improved GPP retrieval with non-nadir views been realized.

Another reason for study-dependent variation in the MODIS-PRI vs. LUE relationship might be attributed to different definitions and approaches for determining LUE (Peñuelas et al., 1995; Chapin et al., 2006; Gitelson and Gamon, 2015). Certainly, while MODIS-PRI values have been successfully related to LUE in a number of studies, there remain uncertainties in the utilization of these relationships because they vary among studies with different vegetation types, different reference bands, different viewing geometry subsets, and which draw upon imagery from only Terra, or from both Aqua and Terra.

2. Objectives

Direct observation of LUE using satellite spectral information could significantly reduce the complexity and uncertainty inherent in highly

parameterized ecosystem models of carbon, water, and energy exchange that are dependent on ancillary meteorological inputs. However, to use MODIS-PRI for estimating LUE over landscapes requires an understanding of how/why the relationship between PRI and LUE varies for different vegetation types, viewing geometries, illumination changes, and which MODIS bands are best used for this purpose. Our objectives are to understand the factors that influence the ability of MODIS-PRI to monitor ecosystem daily LUE when obtained from multiple sites, multiple years, and acquired with both Aqua and Terra. How important are illumination conditions and year to year variations in the use of MODIS-PRI for daily LUE estimations? Does MODIS-PRI differ for Terra vs. Aqua? How influential is the viewing geometry, such as nadir vs. off-nadir observations, on the successful use of MODIS-PRI for LUE and/or GPP estimation, given that the forward scatter and backscatter satellite collections made by Terra and Aqua are displaced from the SPP, missing the maximum/minimum values at the cold spot/hot spot associated with shaded and sunlit foliage sectors? What factors contribute to variation in the MODIS-PRI vs. in situ LUE relationships among sites?

This study begins to address these issues by examining MODIS-PRI derived from both Terra and Aqua satellites during the midsummer seasons of multiple years at four forest sites having different species composition. The overall goal was to develop general relationships between MODIS-PRI and in situ LUE measured by standardized and calibrated flux towers. To focus on the detection of biochemical (i.e., facultative) changes rather than the effects of seasonal leaf area and pigment (constitutive) changes, this study used midsummer periods when there was little expected change in forest leaf area index (LAI), instead of full growing seasons.

3. Methods

3.1. Site descriptions

The MODIS ocean bands used to calculate PRI have nadir fields of view of 1-km. Therefore, candidate study sites must have similar vegetation for a region >1 km surrounding the tower, to enable off-nadir oblique views. Since flux data from the towers should be consistent and comparable among different sites, we chose sites from the Canadian Carbon Program's (CCP) flux tower network. Network flux towers in the CCP use identical cross-calibrated instrumentation and the data are processed using the same algorithms (Coursolle et al., 2006). To examine the effects of differing vegetation types on the PRI responses, sites were chosen that are dominated by different forest types: Douglas fir, black spruce, aspen, and a mixed deciduous-conifer forest. The sites are described below and relevant aspects are summarized in Table 1.

The mature aspen site (SK-OA) is located in Prince Albert National Park, near Prince Albert, Saskatchewan, Canada. This site has a mature trembling aspen (*Populus tremuloides*) overstory with scattered balsam poplar (*Populus balsamifers*) and a hazelnut (*Corylus cornuta*) dominated understory. The aspen trees during our study period were about 80 years old, approximately 20 m in height, with mid-summer LAI values between 1.7 and 2.6, and canopy cover of roughly 90% (Black et al., 1996; Chen et al., 1997; Barr et al., 2004). LUE has previously been successfully estimated at this site from MODIS data, using a new parameter associated with chlorophyll, fAPARchl (Zhang et al., 2009).

The black spruce site (SK-OBS) was also located in Saskatchewan, Canada and was dominated by mature black spruce (*Picea mariana*) with some occurrence of tamarack (*Larix laricina*). The spruce trees were over 100 years old, with tree height around 10 m, canopy cover of approximately 55% and LAI of 3.7–4.0 (Chen et al., 2006). The understory consisted mostly of feather moss (*Pleurozium schreberi*) and Labrador tea (*Ledum groenlandicum*) (Jarvis et al., 1997; Chen et al., 1997). Extensive leaf spectral and photosynthesis data for SK-OA and SK-OBS were acquired during the BOReal-Ecosystem-Atmosphere Study, BOREAS (Middleton et al., 1997) and can be accessed from the Oak Ridge DAAC (https://daac.ornl.gov/).

The Douglas fir site (BC-DF49) is located on the eastern side of Vancouver Island, British Columbia, Canada. During the years of this study, the site consisted of 80% Douglas-fir (*Pseudotsuga menziesii*), 17% western red cedar (*Thuja plicata*) and 3% western hemlock (*Tsuga heterophylla*). Stand density was 1100 stems ha^{-1}, with tree height ranging between 30 and 35 m, and LAI of approximately 8.4 to 9.1 (Morgenstern et al., 2004; Humphreys et al., 2006; Chen et al., 2006). The PRI responses at this site were examined in several tower-based studies (Hilker et al., 2008; Hall et al., 2008; Middleton et al., 2009a; Cheng et al., 2009). The site was subsequently logged in 2011 and replanted.

The mixed forest site (ON-Mix) is located in Ontario, Canada, approximately 80 km southwest of Timmins, near the Groundhog River. The forest regrew following high-grade logging in the 1930s. The site is dominated by five species: trembling aspen (*Populus tremuloides*), black spruce (*Picea mariana*), white spruce (*Picea glauca*), white birch (*Betula papyrifera*), and balsam fir (*Abies balsamea*). In some patches of the forest, eastern white cedar (*Thuja occidentalis*) is also found. Overall, the forest composition is approximately 55% deciduous hardwood and 45% coniferous softwood with LAI of 2–3. Maximum canopy height was ~30 m (McCaughey et al., 2006; Sun et al., 2008).

3.2. Daily in situ LUE at the flux towers

These four sites are all included in the CCP flux tower network, which measures Net Ecosystem Production (NEP) using eddy-covariance methods from towers above the forest canopies. NEP from flux tower measurements was partitioned into GPP and ecosystem respiration using a standardized approach incorporated by the CCP (Barr et al., 2004; Amiro et al., 2006). At all sites, incident and reflected PAR above the canopy along with the PAR transmitted through the canopy

Table 1
Description of the study sites and the daily in situ LUE (mol C mol^{-1} absorbed quanta) determined from the flux towers at those sites. Four Canadian forests were examined: Douglas fir, British Columbia (BC-DF49); mature black spruce, Saskatchewan (SK-OBS); mixed deciduous, Ontario (ON-Mix); and mature aspen, Saskatchewan (SK-OA).

Site ID	N	Location	Latitude/Longitude	Dominant cover type	Observation period	Daily LUE (mol C mol^{-1} absorbed quanta) Mean ± SD	Min/Max
All Sites	420	Canada	48.22°–53.99°N 82.16°W–205.33°W	Boreal Forest	2001–2006	0.0148 ± 0.0056	0.0006/0.0308
BC-DF49	178	British Columbia	49.87°N 125.33°W	Douglas fir	Days 61 to 279, years 2001–2006	0.0164 ± 0.0036	0.0090/0.0294
ON-Mix	123	Ontario	48.22°N 82.16°W	Mixed aspen and spruce	Days 91–262, years 2004–2006	0.0125 ± 0.0063	0.0006/0.027
SK-OA	58	Saskatchewan	53.63°N 106.20°W	Mature aspen	Days 140–249, years 2004–2005	0.0187 ± 0.0068	0.0014/0.03
SK-OBS	61	Saskatchewan	53.99°N 105.12°W	Mature black spruce	Days 140–256, years 2004–2005	0.0113 ± 0.0029	0.0050/0.0184

were measured at/near the towers. From these data *f*APAR was calculated as:

$$fAPAR = (Q_{in} - Q_r - Q_t)/Q_{in} \quad (3)$$

where Q_{in} is the incident PAR, Q_t is the PAR transmitted through the canopy, and Q_r is the PAR reflected from the canopy top (Hipps et al., 1983). Representative in situ *f*APAR values were then calculated for the times of the MODIS overpasses at each site. In this study in situ LUE was calculated based on daily tower measurements. The half hourly values of GPP and incident PAR were integrated to obtain daily values, with LUE calculated as the ratio of the daily GPP to the product of *f*APAR and the daily incident PAR (*f*APAR ∗ PAR). For one aspect of this study, the comparison of same day Terra and Aqua observations, the LUE was determined using the tower measurements corresponding to the satellite overpass times.

LUE was also modeled with the same algorithm used in the Biome Properties Look-Up Table (BLUT) of the MODIS GPP model (MOD17). In that model, a maximum LUE (ε^*) is defined for each biome type, which is reduced by scaling functions driven by daily minimum air temperature and daytime average vapor pressure deficit (VPD), using coefficients assigned by biome type (Heinsch et al., 2003). We calculated a MOD17 LUE from air temperature and VPD values measured at the flux towers, using the parameters defined for each site as assigned in the MODIS land cover classification and used in the MODIS GPP model.

3.3. Satellite viewing geometries: Terra vs. Aqua

In our dataset, observations from Terra and Aqua have distinct patterns of view azimuth angles (VZAs), with view azimuth angles for Terra occurring between 43° to 62° (forward scatter sector) or 232° to 250° (backscatter sector), while Aqua view azimuth angles always fall between 114° to 130° (backscatter view sector) or 300° to 318° (forward scatter view sector) relative to the SPP [Fig. 1]. These differences between observations from the Terra and Aqua satellites are due to differences in their relative azimuth observation angles, a consequence of Terra having a descending daytime orbit (northeast to southwest direction) while Aqua has an ascending daytime orbit (southeast to northwest direction). To examine VZA effects, the combined Terra and Aqua image data (VZA ≤ 45°) were divided into three groups: (i) near nadir views (N), where the VZA is ≤15°; (ii) backscatter views (B), where the VZA is >15° and the view azimuth position relative to the SPP is > 270° (for Terra) or ≤90° (for Aqua); and (iii) forward scatter views (F), where the VZA is >15° and the view azimuth position relative to the SPP is >90° (for Terra) and ≤270° (Aqua). The azimuth relative to true north always differs somewhat from the instantaneous solar azimuth plane (Fig. 1), which varies according to time of day, day of year, and latitude.

Additional key Terra/Aqua differences include time of day for the overpasses, which occur in late morning/early afternoon respectively at the latitudes of our study sites, and the quality of the MODIS instruments (Franz et al., 2008). For data included in this study, Terra overpass times varied between 10:55 and 12:30 local time, while Aqua overpass times varied between 12:45 and 14:15 local time. Note, SK-OBS and SK-OA are on Central Standard Time (CST), BC-DF49 is on Pacific Standard Time (PST), and ON-Mix is on Eastern Standard Time (EST). On average there was approximately a 1 h 45 min difference between the overpass times of the two satellites.

3.4. Extracting and atmospherically correcting MODIS swath data

We examined MODIS data for multiple sites over multiple years from both the Terra and Aqua satellites, using MODIS Collection 5. Although the processing chain for the MODIS land bands (Bands 1–7) includes the production of 8- and 16-day surface reflectance composites of nadir-BRDF adjusted (NBAR) images (Schaaf et al., 2002), corrected to nadir views to minimize surface anisotropy effects (e.g., Huete et al., 2002; Fensholt et al., 2010), this approach has not been adopted for the MODIS ocean bands for data acquired over land. In fact, since the MODIS ocean bands in Collection 5 were never routinely processed to surface reflectance over land regions, we developed our own procedures to calculate surface reflectance for the MODIS ocean band imagery acquired over land at our sites, following the existing atmospheric correction method used for MODIS land bands with the Second Simulation of the Satellite Signal in the Solar Spectrum (6S) program (Vermote et al., 1997, Drolet et al., 2005). Our analyses utilized individual acquisitions and not temporal composites.

We focused this study on the effects of photosynthetic down-regulation on productivity, rather than the effects of varying green LAI (and *f*APAR) since PRI has been shown to vary with LAI (Barton and North, 2001). Therefore, we identified time periods when little change in LAI was expected, by examining seasonal NDVI patterns in MODIS data acquired for each site. NDVI was computed using MODIS land bands, Bands 1 (620–670 nm) and 2 (820–870 nm). During periods of the growing season where NDVI showed little change, a list of clear days was generated by comparing the expected incident PAR, based on the seasonal change in solar elevation, with the incident PAR observed at the flux towers. Clear days were defined as those where the expected and observed incident PAR were within 15%. MODIS observations with VZAs >45° were rejected to reduce noise due to spatial integration of the radiance signal over large areas, and especially to constrain the views to our specific study areas. We utilized MODIS Band 1 and five of the 10 nm ocean bands: Band 10 (483–493 nm), Band 11 (526–536 nm), Band 12 (546–556 nm), Band 13 (662–672 nm), and Band 14 (673–683 nm). The 250-m land bands were averaged to produce pixels equal to the 1-km ocean bands.

The MODIS at-sensor radiance (MOD021KM) and aerosol optical thickness (MOD04) data were subset to create a smaller region around each flux tower and merged. These data were atmospherically corrected to surface reflectance using the 6S program (Drolet et al., 2005; Vermote et al., 1997) and surface reflectance values for the field of view that included the flux tower were matched with in situ LUE values from those towers. Observations with low NDVI (NDVI < 0.19) were removed, under the assumption that low NDVI values were due to either low LAI or snow in the scene. We obtained a total of 420 satellite scenes that paired MODIS reflectance with tower flux measurements. For BC-DF49 there were 178 observations in years 2001–2006 for days of the year (DOY) 61–279; for ON-Mix there were 123 observations in years 2004–2006 for DOY 91–262; for SK-OA there were 58 observations for DOY 140–249 in years 2004–2005; and for SK-OBS there were 61 observations for DOY 140–256 in years 2004–2005 [Table. 1].

3.5. Obtaining MODIS-PRI and relating to in situ LUE

In the calculation of MODIS-PRI, MODIS Band 11, encompassing the physiologically active wavelength at 531 nm, was paired with five different reference bands to evaluate their performance for association with daily tower LUE. These reference band candidates were four of the narrow (10 nm) ocean bands: Band 10 (blue), Band 12 (green), two contiguous red bands (Band 13, Band 14) – and the wide (50 nm) land Band 1 (red). To designate the bands used in the calculation of MODIS-PRI variations, band numbers were listed in parentheses with the reference band put first. For example, PRI(10,11) paired the reference Band 10 with the active band (Band 11).

The various MODIS-PRIs at each of the four study sites per date (DOY, year) were combined with the available information associated with the MODIS sensors (Terra, Aqua) and MODIS viewing geometries (e.g., VZA; view azimuth angle; and azimuth angle relative to the sun, RelAZ) and with flux tower information (e.g., incident PAR, fAPAR, GPP, daily LUE, surface temperature, humidity). We examined the relative ability of each of these MODIS-PRI versions to describe daily tower LUE overall, and at each study site. We also derived an empirical PRI-

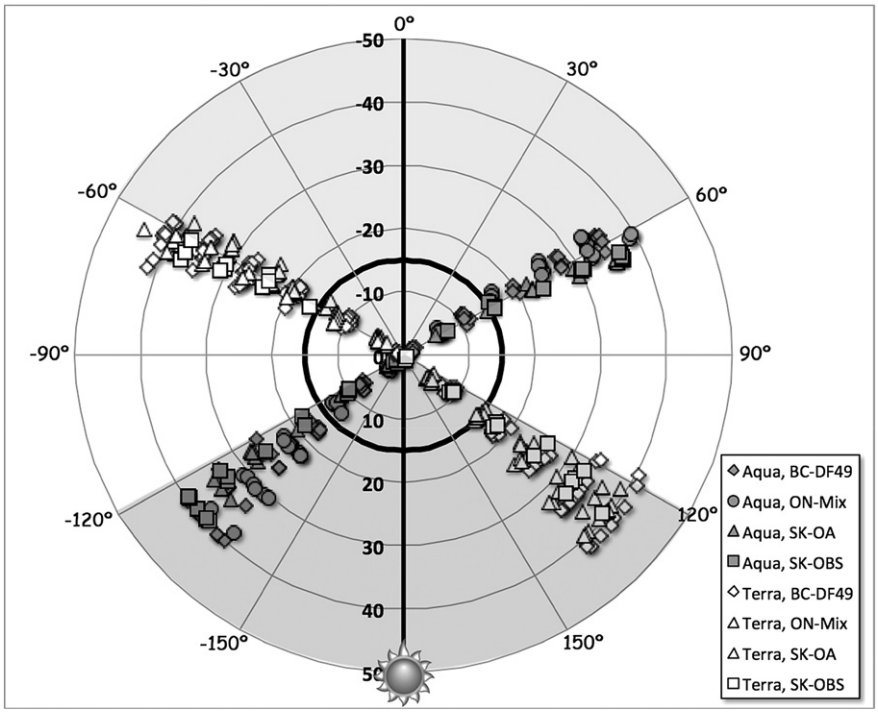

Fig. 1. This polar plot of MODIS relative viewing geometry for data used in this study. It shows view zenith angles (VZAs, concentric rings) and view azimuth angles (radial lines along outside ring) relative to the solar principal plane (SPP, the plane defined as 0° to 180° along the sun's illumination path) at the time of satellite overpass. VZAs are given as the radial distance from the center. The dark circle indicates the 15° VZA, which encloses views considered to be "nadir" (VZA ≤ 15°) in the analysis. The backscatter VZAs have negative values (−15° to −45°) and fall along the view azimuths close to ±60° of the SPP (120°, Aqua; 240°, Terra), and are shown in the top half of the polar plot. Forward scatter VZAs have positive values (15° to 45°) and fall along view azimuths within ±60° of the SPP (Terra, between 45° and 60°; Aqua, between 300° and 330°), and are shown in the bottom half of the polar plot. MODIS daylight data are collected when Terra is in the descending node of the orbit, while Aqua daylight data are collected in its ascending node. MODIS scans the Earth's surface along a swath that is perpendicular to the orbital ground track. The difference between the planes of the satellite ground tracks at the latitude of these sites causes the alignment of the view azimuth angles into the two different lines.

based LUE (PRI-LUE), using regression equations developed at each site. We utilized the operational MODIS GPP (MOD17) model (Heinsch et al., 2003) to directly compare MOD17 LUE with in situ LUE and to provide a baseline for comparison with LUE derived from various MODIS-PRI subsets.

Since MODIS does not have the critical narrow spectral bands necessary to compute many published pigment indices related to chlorophyll and carotenoid content (e.g., Peñuelas et al., 1994), we could only pursue use of one spectral index for estimates of upper canopy carotenoid content, as a modification of the Carotenoid Reflectance Index [CRI = (1/R510)–(1/R550)] (Gitelson et al., 2002) using ocean Bands 10 (488 nm) and 12 (551 nm).

Statistical analyses were accomplished using Systat 13 (Systat Software, San Jose, CA 95110). Various regression models were investigated using Analysis of Variance (ANOVA) and General Linear Model (GLM) approaches with the full dataset and subsets for each site, satellite, and view geometry group.

4. Results

We evaluated different approaches for the calculation and utilization of MODIS-PRI to determine daily tower LUE, examining this possibility for several scenarios for: (i) the combination of all sites with both satellites; (ii) individual sites; (iii) each satellite; and (iv) separate view geometry subsets. Our evaluations began by examining the use of different reference bands in the PRI calculation (Eq. 2). We continued our study using the highest overall performing MODIS-PRI version in estimating daily LUE. We used a statistical approach that allowed us to consider site differences, illumination conditions (PAR; fAPAR; dates of acquisition, DOY & year, and solar zenith angle, SZA), the effects of MODIS viewing geometries, and the differences between MODIS-PRI derived from data collected by Terra (AM) vs. Aqua (PM).

4.1. Study sites

Daily LUE determined at the flux towers varied over the observed time periods, with distinct differences among sites [Table 1]. Even though we specifically chose summer periods without significant variations in LAI or expected pigment shifts, there was a wide range in observed LUE, with values ranging from a low of 0.0006 to a high of 0.0308 mol C mol^{-1} absorbed quanta [Table 1]. The sites had significantly different LUE means (ANOVA, $p < 0.01$): SK-OA had the highest, followed by BC-DF49, whereas SK-OBS had the lowest mean LUE. The within-site temporal variability of LUE also differed among sites, with the coniferous sites (BC-DF49 and SK-OBS) having much lower standard deviations (SD) than the aspen and mixed forest sites [Table 1].

4.2. MODIS-PRI versions computed with different reference bands

The means, SDs, and ranges were computed for the NDVI and each of the 5 possible versions of MODIS-PRI, which are summarized in Table 2. The MODIS-PRI values for all MODIS scenes (n = 420) that resulted from these five MODIS band combinations show that their computed averages are very different, as are their ranges. The values typically produced by the standard PRI (based on a reference wavelength at 570 nm) typically range between ±0.2. The only version of MODIS-PRI that provides values in that range are obtained with MODIS-PRI(12,11) using the second green (550 nm) band. Hereafter we refer to this as PRI(12,11), and apply this simpler format to the other versions. The PRI(12,11) provided values that consistently fell below zero (mean = −0.095; range, −0.013 to −0.505), as might be expected by comparison with previous remote sensing studies that used this MODIS-PRI version at three of these sites (Hall et al., 2008; Drolet et al., 2005, 2008; Middleton et al., 2009a; Cheng et al., 2009), and

Table 2
The means and ranges of PRI values are provided, when computed with MODIS Band 11 and five different MODIS reference bands. Each PRI is listed with the MODIS Band 11, an ocean band associated with the physiologically active wavelength at 531 nm, and the band number used for the reference. Also listed is the normalized difference vegetation index (NDVI) using MODIS land Bands 1 and 2.

	NDVI	PRI(1,11)	PRI(10,11)	PRI(12,11)	PRI(13,11)	PRI(14,11)
N of cases	420	420	420	420	420	420
Minimum	0.193	−0.21	−0.025	−0.505	−0.625	−0.639
Maximum	0.935	0.363	1.138	−0.013	0.364	0.39
Arithmetic mean	0.716	0.095	0.222	−0.095	0.074	0.075
Standard deviation	0.138	0.099	0.131	0.051	0.157	0.158

which fall in a value range suggesting mild to moderate physiological stress across these forests.

The three MODIS-PRI versions that used reference bands in the red spectral region showed strong correlations to each other; since the correlation between PRI(1,11) and PRI(14,11; r = 0.84) and PRI(13,11; r = 0.82) were similar, these two MODIS-PRIs computed with the red ocean bands (13 or 14) were highly correlated (r = 0.98). All of these significant correlations ($p \leq 0.000$) required inclusion of a site-specific term (Site ∗ PRI); this term accounted for 8–10% of the variance in the correlation between PRI(1,11) vs. PRI(13 or 14,11) but described a much larger fraction (67%) of the variance in the correlation between PRI(1,11) vs. PRI(10 or 12,11). Therefore, the three MODIS-PRIs computed using red reference bands had much less site-related influences overall than those computed with reference Bands 10 or 12.

4.3. Regression analyses based on MODIS-PRI versions

The different MODIS-PRI versions were initially evaluated for relative usefulness in remote monitoring of surface LUE dynamics of forests by combining all available MODIS data per site and comparing single factor linear regressions for each of the MODIS-PRIs vs. daily LUE; the coefficients of determination (r^2 values) are summarized for all observations combined as well as per site in Table 3. For each site individually as well as for all points combined, the PRI(1,11) had the highest associations with daily LUE in terms of r^2 values and lowest root mean square errors (RMSE), all of which were significant ($p \leq 0.05$). This successful use of the MODIS red land band as the reference is consistent with the results reported by Goerner et al. (2009). However, this one-factor analysis only explained 33% of the overall variation in MODIS-PRI across sites, although a better individual site result was achieved for the ON-Mix site ($r^2 = 0.565$) (Table 3). Results were similar for the two MODIS-PRIs based on the narrow red bands (either PRI(13,11) or PRI(14,11)), but were less successful than the broad red band. In contrast to the studies reported by Drolet et al. (2005, 2008) that only used data from the Terra morning satellite, the relationships between either PRI(10,11) or PRI(12,11) and LUE had the worst coefficients of determination ($r^2 \leq 0.17$) of all of the MODIS-PRI versions tested. However those previous studies by Drolet et al. (2005, 2008) included a broader seasonality and larger view angle range. Given the stronger performance of PRI(1,11) as compared to the four other PRI versions, we conducted our further analyses with this index.

Table 3
The overall simple regression between the PRI (the dependent variable) calculated using different reference bands, band numbers indicated in parentheses, and daily in situ LUE (the independent variable) for all observations obtained at the four individual study sites with the ANOVA model. The coefficient of determination (r^2) describes the relative amount of variation in the PRI values that is explained by the independent variable (Daily LUE). Bold numbers are $r^2 > 0.30$. The PRI(1,11) had the strongest relationship to Daily LUE. Four Canadian forested sites are examined (Douglas fir, British Columbia; mature black spruce, Saskatchewan; mixed deciduous, Ontario; and mature aspen, Saskatchewan).

Site	N	PRI(10,11) r^2	PRI(12,11) r^2	PRI(13,11) r^2	PRI(14,11) r^2	PRI(1,11) r^2
All points	420	0.04	0.001	0.209	0.22	**0.326**
BC-DF49	178	0	0.005	0.052	0.052	0.073
ON-mix	123	0.169	0.011	**0.363**	**0.363**	**0.565**
SK-OA	58	0.013	0	0.129	0.186	**0.334**
SK-OBS	61	0	0.031	0.046	0.084	**0.356**

4.4. Using PRI(1,11) for daily LUE at study sites

The statistics describing simple relationships between PRI(1,11) and daily in situ LUE for the four sites, merging all observed view angles and both satellites, are provided in Table 4. As noted in Table 3 for all data taken together, there is a general, but noisy, trend, with higher values of PRI(1,11) associated with higher values of LUE ($r^2 = 0.33$, RMSE = 0.0046 mol C mol^{-1} absorbed quanta, $p < 0.05$, Fig. 2A). However, each site displayed a different relationship between PRI(1,11) and daily LUE within the full dataset [Fig. 2B]. The two coniferous sites, BC-DF49 and SK-OBS, had the smallest slopes that while overlapping within their 90% confidence intervals, still had a significant offset between them. Both the slopes and intercepts for the aspen and mixed sites fell within the 95% confidence intervals, with the mixed site slope having a value between that of the aspen and spruce, as expected.

Although the sites had similar ranges in PRI(1,11) values, the coniferous sites displayed much less variation in LUE than either the aspen or the mixed site. The site RMSE values ranged from 0.0023 (SK-OBS) to 0.0056 (SK-OA) mol C mol^{-1} absorbed quanta. The average RMSE for all sites combined was 0.0046 mol C mol^{-1} absorbed quanta. We adjusted for site differences by applying the regression equations for each site [Table 4] to estimate LUE based only on PRI(1,11), producing our data-derived modeled variable designated as PRI-LUE. Accounting for site differences using PRI-LUE yielded an improved correlation between MODIS-derived LUE predictions and in situ LUE observations over all sites (r = 0.72), although the modeled PRI-LUE for BC-DF49 exhibited a threshold at LUE > 0.012 mol C mol^{-1} absorbed quanta [Fig. 3].

We note that these initial analyses examined regressions describing the dependence of the PRI(1,11) on in situ LUE, without consideration of other influential factors.

4.5. GLM analyses of the full dataset

We examined all available data (n = 420) with a General Linear Model (GLM) to obtain the most generalized results for analysis of PRI(1,11), whereby the combined effects of other contributing factors were considered together. The main effects in this analysis included two category variables (Site and Satellite), and several continuous

Table 4
Descriptions of statistical parameters obtained from linear regressions between PRI(1,11) and daily LUE using ANOVA, for all observations obtained at the four individual study sites (see Fig. 2). The coefficient of determination (r^2) describes the relative amount of variation in the PRI values that are explained by the independent variable (daily in situ LUE). Units for the root mean square error (RMSE) are mol C mol^{-1} absorbed quanta.

Site	N	Intercept	Slope	P≤	r^2	RMSE
All points	420	−0.055	11.315	0.000	0.326	0.0060
BC-DF49	178	−0.002	6.610	0.000	0.073	0.0035
ON-Mix	123	−0.113	13.484	0.000	0.565	0.0041
SK-OA	58	−0.001	7.230	0.000	0.334	0.0056
SK-OBS	61	−0.106	17.571	0.000	0.356	0.0023

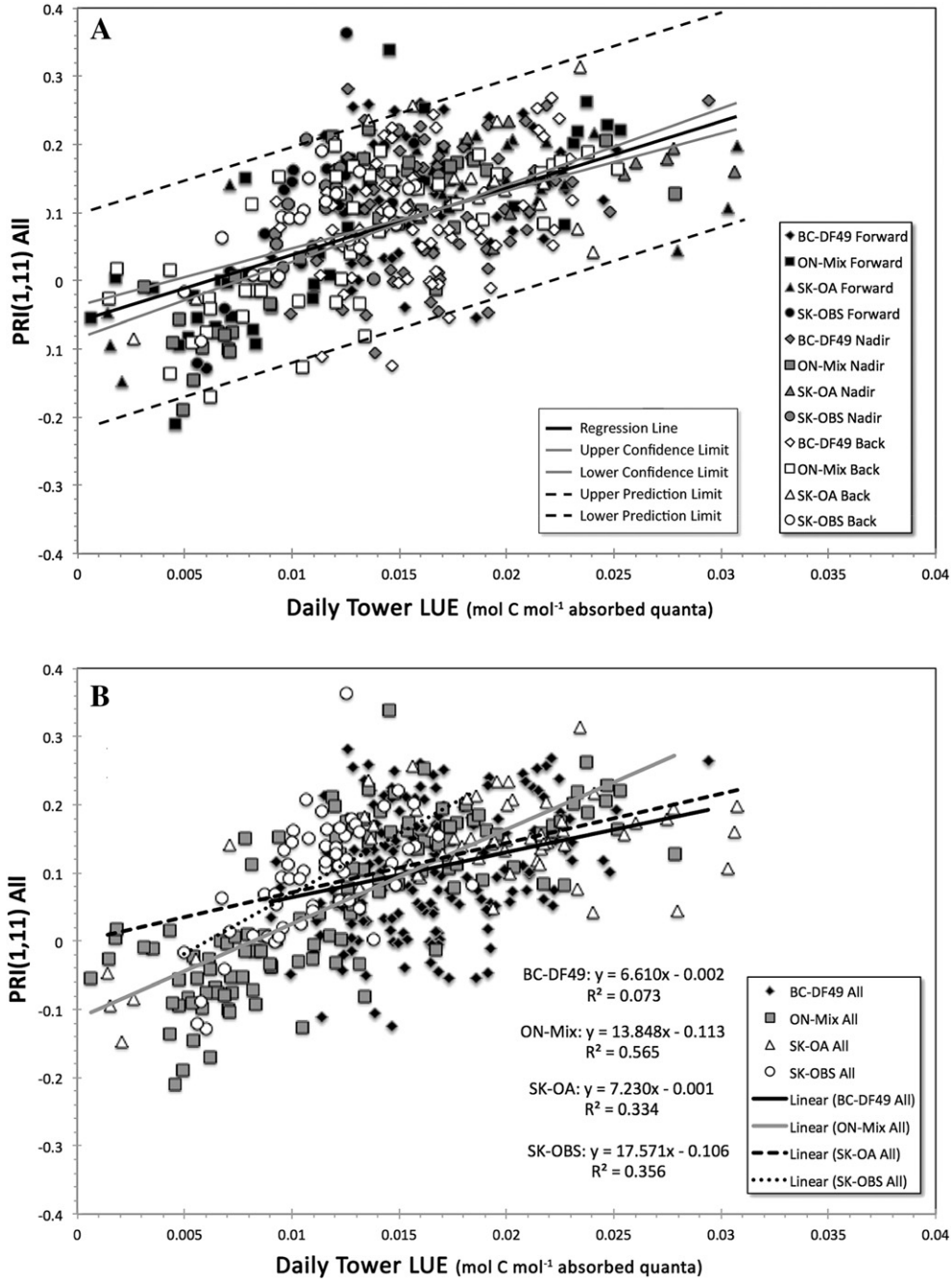

Fig. 2. PRI(11,1) vs. daily in situ LUE from flux towers over multiple growing seasons, for four Canadian forested sites, two MODIS satellite sensors (Terra, Aqua) and all available view geometries. [A] All points: Equation: $y = 10.182x - 0.056$ ($r^2 = 0.324$; RMSE = 0.007; $p < 0.000$; $n = 420$). When sites are added as a category variable, a small gain in overall agreement is achieved: Equation: $y = 11.315x - 0.055$ ($r^2 = 0.383$; RMSE = 0.006; $p < 0.000$; Site means and slopes are significant, $p < 0.000$; $n = 420$). [B] Linear regression lines for each of the four study sites are added. Site means and slopes are significant, $p < 0.000$; $n = 420$). Symbols, line types, RMSE (mol C mol^{-1} absorbed quanta) and regression equations per site are given. See Table 4 for the regression equations.

variables (Daily LUE, Year, DOY, incident PAR, VZA, RelAZ, SZA, and the carotenoid pigment index). This analysis of the full dataset provided a 27% increase in the variation explained for PRI(1,11) as a function of LUE ($r^2 = 0.60$, $p \leq 0.000$, $n = 420$; Table 5A), as compared with the previously described one-factor (LUE) regression ($r^2 = 0.33$, RMSE = 0.0046, Table 4). With this multi-factor approach, daily LUE explained the largest portion of the Sums of Squares (F-$Ratio_{LUE} = 52.37$) and lower error was achieved (RMSE = 0.004 mol C mol^{-1} absorbed quanta), thereby revealing a stronger dependency of MODIS-PRI on daily LUE when other influential factors were simultaneously considered. A simplified version of the Analysis of Variance Table (ANOVA) for the full dataset is provided [Table 5A].

This GLM analysis revealed some of the complexity and confounding factors that affect the relationship between MODIS-PRI and LUE. For the full dataset [Table 5A], Site differences were significant ($p = 0.032$) and four other highly significant variables ($p \leq 0.001$) were either indirectly related to illumination (DOY, Year) or directly related to illumination (PAR_{in}, fAPAR), indicating that seasonality within the summertime periods examined and year to year differences contributed to variations in the observed PRI(1,11) values. Three 2-factor interaction terms describing site differences were also significant: Site * LUE ($p = 0.015$), Site * PAR_{in} ($p = 0.005$), and Site * Satellite ($p = 0.003$, not included in Table 5), The statistically non-significant factors (ns) in the full dataset analysis were: satellite, SZA, VZA, view azimuth angle, relative

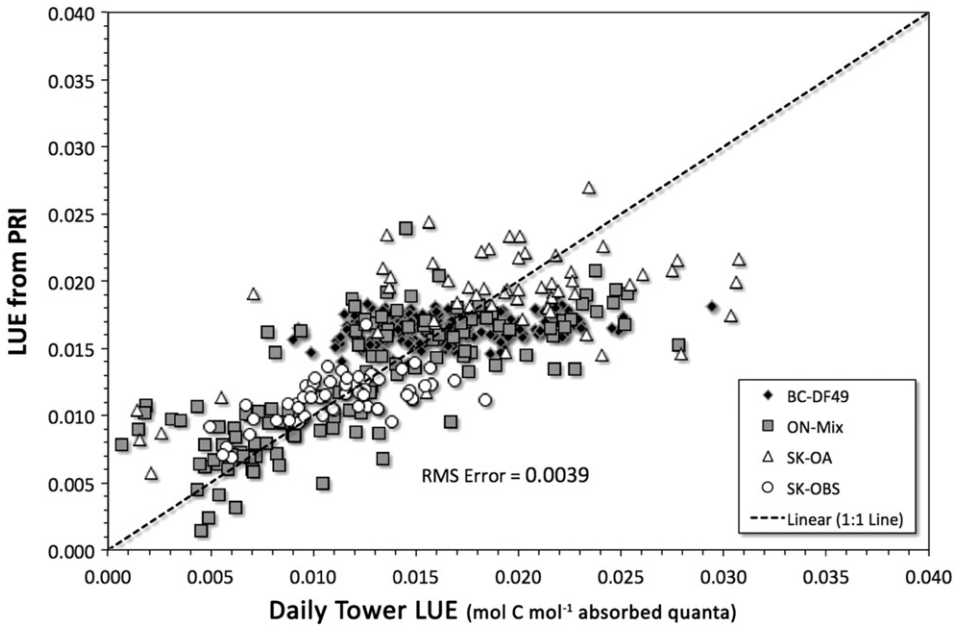

Fig. 3. The modeled variable PRI-LUE (mol C mol^{-1} absorbed quanta) provides an estimate of daily flux tower LUE (mol C mol^{-1} absorbed quanta) for all points (n = 420) is shown with the 1:1 line (correlation coefficient, r = 0.52; RMSE = 0.00391 mol C mol^{-1} absorbed quanta). PRI-LUE was derived from PRI(1,11) by adjusting for site differences using the regression equations presented in Fig. 2B and Table 4. Symbols represent data from the four Canadian forest sites: black diamonds for BC-DF49, gray squares for ON-Mix, unfilled triangles for SK-OA, and unfilled circles for SK-OBS.

view azimuth, carotenoid pigment index, and additional interaction terms.

The overall variability among sites, view geometries, and MODIS sensors is portrayed with the box plots in Fig. 4A and a bar chart in Fig. 4B. It is apparent that nadir and forward views produced higher PRI(1,11) values for Terra than for Aqua in general, while Terra vs. Aqua comparisons for backscatter views were variable (Fig. 4B). We also found that the average PRI(1,11) values were significantly higher when collected from Terra vs. Aqua, for three of four sites – all except the SK-OA site where values per satellite were the same (Fig. 4B), but that the distribution of data points per site and view subgroup overlapped, as indicated with box plots (Fig. 4A). This complex situation suggests that drawing on MODIS data to examine our primary hypothesis (Eq. 1) by using MODIS-PRI as a surrogate for LUE requires us to examine this relationship separately for Terra vs. Aqua and/or for different viewing geometries, and that site differences matter.

Table 5
Summary of statistics for significant factors in GLM analysis: PRI(1,11) vs. Daily Tower LUE and other main effect variables. All data (n = 420 MODIS scenes) are included: A] no subgroups; B] subsets by Site, for the four Canadian forested sites (Douglas fir in British Columbia; mature black spruce in Saskatchewan; mixed deciduous in Ontario; and mature aspen in Saskatchewan). C] subgroups by view direction (forward scatter, nadir, and backscatter). The first three rows provide the statistical summary terms (N; r^2, coefficient of determination; RMSE; and F-$ratio_{LUE}$). The next section (13 rows) provides the significance level (p-values) for the main effect variables and two interaction terms. The term "n/a" means "not applicable" and "ns" means "not significant."

GLM statistics		5A	5B				5C		
		All data	Subsets by sites				Subsets by view direction		
Summary			BC-DF49	SK-OBS	ON-Mix	SK-OA	Forward	Nadir	Back
N		420	178	61	123	58	154	118	148
r^2		0.60	0.42	0.69	0.76	0.67	0.69	0.62	0.54
RMSE		0.004	0.005	0.003	0.004	0.003	0.004	0.005	0.005
F-$ratio_{LUE}$		52.37	7.42	0.11	5.49	12.17	32.75	19.51	10.87
Variables	Variable type				Probability (p) values				
LUE	Tower	0.000	0.007	ns	0.021	0.000	0.000	0.000	0.001
Site	Site	0.032	n/a	n/a	n/a	n/a	0.009	0.001	ns
Satellite	Satellite	ns	ns	ns	ns	0.053	ns	ns	ns
Year	Date/Illumination	0.000	0.000	ns	ns	ns	0.001	0.024	0.015
DOY	Date/Illumination	0.000	0.002	0.000	0.000	ns	0.000	0.069	0.003
PAR	Illumination	0.001	0.015	ns	0.013	ns	ns	0.002	0.038
fAPAR	Illumination	0.000	0.001	ns	0.005	ns	0.008	0.000	0.001
SZA	Illumination	ns	ns	0.000	0.087	ns	ns	ns	ns
VZA	View geometry	ns	ns	ns	ns	ns	ns	0.108	ns
VAA	View geometry	ns	ns	ns	ns	0.074	ns	0.035	ns
RelAZ	View geometry	ns	ns	ns	ns	ns	ns	ns	ns
CRI	Pigment	0.092	ns	0.053	ns	ns	ns	ns	ns
Site * LUE	Interaction	0.015	n/a	n/a	n/a	n/a	0.013	ns	ns
Site * PAR	Interaction	0.005	n/a	n/a	n/a	n/a	0.006	ns	ns
No. of significant variables (p ≤ 0.05)		8	5	3	4	2	7	6	5

* N (sample size); RMSE (root mean square error), F-$Ratio_{LUE}$ (F-Ratio for the LUE variable).
** Light Use Efficiency (LUE), PAR (photosynthetically active radiation), fAPAR (fraction of absorbed PAR), view zenith angle (VZA), view azimuth angle (VAA), VAA relative to the solar principal plane (RelAZ), and carotenoid reflectance index (CRI).

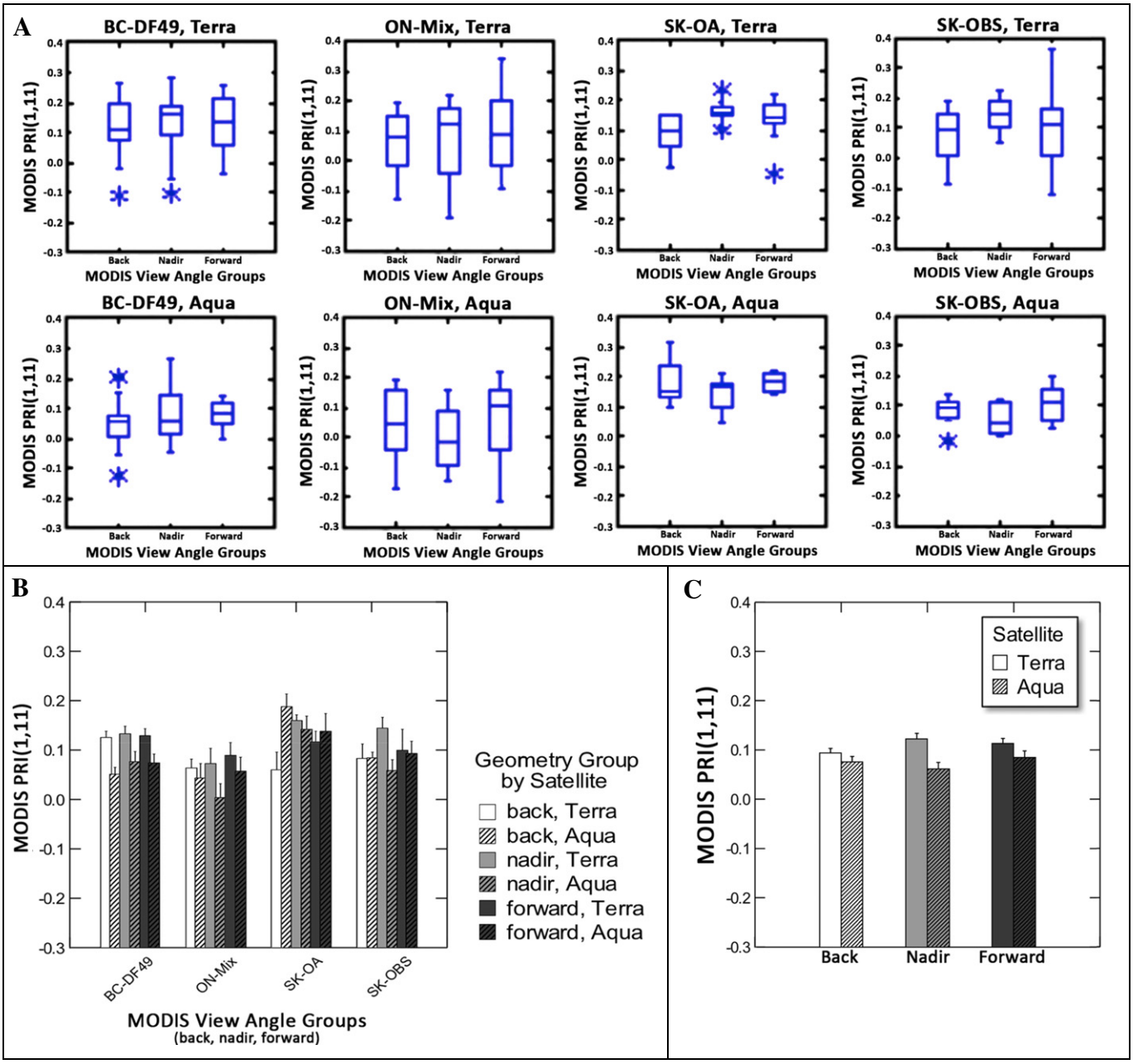

Fig. 4. [A] Box plots for the view angle groups (backscatter, nadir, and forward scatter) separately by satellite: Terra (top row) and Aqua (bottom row) and sites (columns). The center horizontal line in each box marks the median of the sample, and the box length shows the central 50% range for values. The asterisk indicates data that fall outside of the 50% range. [B] The variability of MODIS PRI(1,11) for the four forested sites. The mean (± Standard Error, SE) for Terra (T, solid bar, morning) and Aqua (A, stripped bar, afternoon) per site and view angle groups (backscatter, nadir, and forward scatter), where the sequence of bars for each site is: $(T, A)_{back}$, $(T, A)_{nadir}$, and $(T, A)_{forward}$. [C] The MODIS PRI(1,11) values were averaged over the four study sites, separately for Terra and Aqua by view angle group. The Terra (morning) values were higher than Aqua (afternoon) for all view angle subgroups, but significant differences ($p < 0.01$) were revealed for nadir and forward scatter values – Terra values were always greater than Aqua (T > A).

4.6. GLM analyses of individual sites

Next, we examined the study sites separately [Table 5B]. The ON-Mix site produced the strongest relationship of PRI(1,11) to LUE ($r^2 = 0.76$; RMSE = 0.004 mol C mol^{-1} absorbed quanta; F-$Ratio_{LUE} = 5.49$; n = 123). However, three illumination-related differences (DOY, PAR, and fAPAR) were all highly significant ($p \leq 0.013$) at this mixed deciduous site. The SK-OA site had the next strongest results ($r^2 = 0.67$; RMSE = 0.003 mol C mol^{-1} absorbed quanta; F-$Ratio_{LUE} = 12.17$; n = 58) and notably LUE was the only significant variable ($p < 0.000$). At the SK-OBS site, SZA replaced LUE as the primary significant illumination factor along with DOY, which together gave an $r^2 = 0.69$ (RMSE = 0.003 mol C mol^{-1} absorbed quanta; n = 61. The BC-DF49 had the least successful results ($r^2 = 0.42$; RMSE = 0.005 mol C mol^{-1} absorbed quanta; F-$Ratio_{LUE} = 7.42$ n = 178); the four illumination-related variables (but not SZA) were all significant ($p \leq 0.015$).

4.7. GLM analyses of 3 viewing geometry subsets

Next, for both satellites combined and all four sites [Table 5C], we examined 3 subgroups of the dataset defined by the viewing geometry (forward (F), nadir (N), and back (B) views) averaged over the available view azimuths, as described earlier. We found that the PRI(1,11) relationship to daily LUE for these view geometry subgroups was equal to, or stronger than, previous results obtained for the full dataset [Table

5C vs. 5 A]: (i) forward scatter ($r^2 = 0.69$; RMSE = 0.004 mol C mol^{-1} absorbed quanta; F-$Ratio_{LUE}$ = 32.75; n = 154); (ii) nadir ($r^2 = 0.62$; RMSE = 0.005 mol C mol^{-1} absorbed quanta; F-$Ratio_{LUE}$ = 19.51; n = 118); and (iii) backscatter ($r^2 = 0.54$; RMSE = 0.005 mol C mol^{-1} absorbed quanta; F-$Ratio_{LUE}$ = 10.87; n = 148). Clearly, the combined Terra/Aqua forward scatter collection had the strongest performance of these three geometry subgroup (F, N, B), and explained an additional 7–15% of the variability in the PRI(1,11) to LUE relationship, as compared to N or B subgroups. In this combined Terra/Aqua forward scatter subgroup, the two variables describing acquisition dates were highly significant (year, DOY), as was fAPAR ($p = 0.008$); two interaction terms were also significant: Site ∗ daily LUE ($p = 0.013$) and Site ∗ PAR ($p = 0.006$). For individual sites, the highest r^2 values occurred with forward scattered subsets for all sites except BC-DF49, which had its best performance for backscatter views.

For nadir views in the combined Terra/Aqua collection [Table 5C], the Site and three illumination-related variables (Year, PAR, fAPAR) were all significant ($p \leq 0.003$). Similar to the forward and nadir combined Terra/Aqua subsets, the backscatter subset showed no difference in the PRI(1,11) discrimination between satellites but illumination-related variables were significant factors (Year, DOY, fAPAR, PAR, $p \leq 0.04$).

One of the most important findings of this view geometry analysis was to confirm that the PRI(1,11) was significantly higher for Terra than for Aqua across sites, when associated with forward scatter ($p = 0.004$) and nadir ($p = 0.002$) subsets [Fig. 4C].

4.8. GLM analyses for separate geometry subgroups for Terra and Aqua

We examined the geometry subgroups (F, N, B) separately within each satellite dataset (Terra, Aqua) [Table 6] and [Fig. 5A–F]. The relationships between MODIS PRI(1,11) and the independent variable, the daily in situ LUE at the towers, were linear when combined across the four study sites, for four of the six relationships (F, N, B for both Terra and Aqua) shown in Fig. 5. The dependence of MODIS PRI(1,11) on the primary LUE independent variable was moderate for the Aqua nadir subset ($r^2 = 0.48$, Fig. 5B) but relatively weak ($r^2 = 0.27$–0.38) for the Aqua backscatter (Fig. 5C) and all three Terra directional subsets (Figs. 5D–F).

We found that the Aqua forward scatter data (Fig. 5A), describing a non-linear function, were superior to other geometry subgroups or site groups for relating PRI(1,11) to daily LUE, but could have been approximated with a linear function. The linear model for the Aqua forward scatter subset (Table 6), had the smallest error term of any subset ($r^2 = 0.83$; RMSE = 0.003 mol C mol^{-1} absorbed quanta; F-$Ratio_{LUE}$ = 15.43; n = 54),. and in addition to LUE ($p \leq 0.000$), there was only one other significant variable, DOY ($p = 0.004$; Table 6). Although the Terra forward scatter subset had nearly twice as many observations as Aqua, it explained 16% less variability, and had three significant ($p \leq 0.013$) illumination related variables (Year, DOY, and fAPAR). However, we note that the Terra forward subset [Table 6] ($r^2 = 0.67$; RMSE = 0.005 mol C mol^{-1} absorbed quanta; F-$Ratio_{LUE}$ = 7.66; n = 100) was just as successful as the combined Terra/Aqua forward scatter collection previously described above [Table 5C].

The Terra vs. Aqua nadir collections across sites [Table 6] provided similar overall results to each other (r^2, 0.65–0.67; RMSE = 0.004; F-$Ratio_{LUE}$ = 8–9), although the Aqua nadir subset was preferred because LUE was the only significant variable ($p = 0.006$). Both the Terra nadir and backscatter subsets were significantly influenced by fAPAR ($p \leq 0.001$). The Aqua backscatter subset for PRI(1,11) had the least successful performance ($r^2 = 0.59$, RMSE = 0.004). Terra nadir and backscatter views for the combined sites yielded similar results (r^2 ~ 0.67, RMSE = 0.004, F-$Ratio_{LUE}$ ~ 8–12, Table 6).

4.9. Simplified GLM analyses for Aqua and Terra: PRI(1,11) vs. LUE

Given that the GLM analyses indicated significant differences among sites and geometry subgroups, a simple linear model to estimate PRI(1,11) as a function of LUE was performed using only these variables: LUE, site, site ∗ LUE [Table 7]. The linear model performed very well for the Aqua forward subset [$r^2 = 0.75$; RMSE = 0.003 mol C mol^{-1} absorbed quanta; F-$Ratio_{LUE}$ = 32.24; $p \leq 0.000$], almost as well as the Aqua forward subset in the full model [$r^2 = 0.83$, Table 6], but here the Site variable were not significant (compare with Table 5C). For this Aqua forward subset, a slightly stronger performance was gained using a non-linear model ($r^2 = 0.79$; RMSE = 0.003 mol C mol^{-1} absorbed quanta; F-$ratio_{LUE}$ = 27.64; $p \leq 0.000$). The Aqua forward subset (from Fig. 5A) was overlaid on the full dataset [Fig. 6] for comparison of the data ranges. This figure clearly shows that the Aqua forward subset from four sites was much less variable than the other data contributing to the full dataset, which included Terra observations and those from nadir and backscatter directions.

Neither the Aqua backscatter nor nadir subsets [Table 7] performed comparably well [r^2, 0.54–0.56; RMSE = 0.004–0.005 mol C mol^{-1} absorbed quanta; F-$ratio_{LUE}$ = 3–4] to the Aqua forward subset across sites. For the Aqua nadir subset, LUE was barely a significant factor

Table 6
Summary of statistics for significant factors in GLM analysis: PRI(1,11) vs. Daily Tower LUE and other main effects. Data were analyzed in view observation subsets (forward scatter, nadir, and backscatter), separately for Terra and Aqua. Terms are defined in Table 5 footnote. The three bold values show that the best results are for Aqua (highest r2, lowest RMSE, best F-ratio(LUE)) and the highly signficant result ($p < 0.01$) for LUE.

GLM statistics		All forward views		All nadir views		All backscatter views	
Summary		Terra	Aqua	Terra	Aqua	Terra	Aqua
N		100	54	68	50	86	62
r^2		0.67	**0.83**	0.67	0.67	0.68	0.59
RMSE		0.005	**0.003**	0.004	0.004	0.004	0.004
F-$ratio_{LUE}$		7.66	**15.43**	8.62	8.88	11.82	15.43
Variables				Probability (p) values			
LUE	Tower	0.007	**0.000**	0.038	0.006	0.001	0.026
Site	Site	ns	0.066	**ns**	ns	ns	0.054
Satellite	Satellite	n/a	n/a	n/a	n/a	n/a	n/a
Year	Date/illumination	0.004	ns	ns	ns	0.101	ns
DOY	Date/illumination	0.000	0.004	ns	ns	0.110	0.042
PAR	Illumination	ns	ns	0.000	ns	ns	ns
fAPAR	Illumination	0.013	ns	0.000	ns	0.001	ns
VZA	View geometry	ns	ns	ns	ns	ns	ns
VAA	View geometry	ns	ns	ns	ns	ns	ns
Rel_AZ	View geometry	ns	ns	ns	ns	ns	ns
CRI	Pigment	ns	ns	ns	ns	ns	ns
Site ∗ LUE	Interaction	ns	ns	ns	ns	0.008	ns
Site ∗ Rel_AZ	Interaction	ns	0.029	ns	ns	ns	ns
No. of significant variables ($p \leq 0.05$)		4	3	3	1	3	2

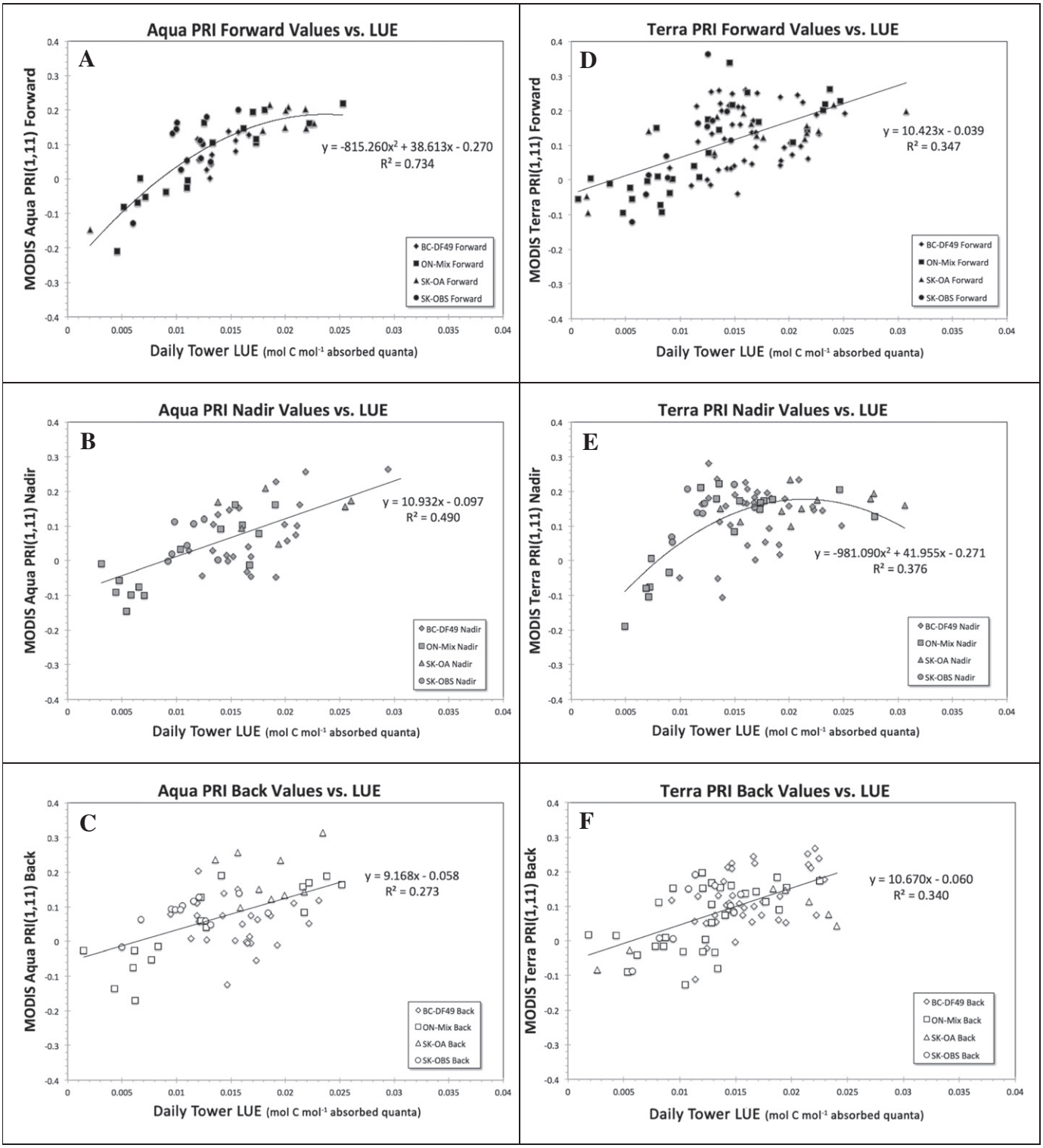

Fig. 5. The regression plots from GLM analyses relating MODIS PRI(1,11) to daily in situ LUE at the towers, for the four study sites: Aqua, A-C; Terra, D-F. Refer to Table 7 for regression equations. [A] Aqua forward scatter subgroup, $r^2 = 0.722$ with power function ($n = 50$; RMSE $= 0.005$; $Fratio_{LUE} = 64.72$; $p \leq 0.001$, 4 statistical outliers removed). Equation: $y = 38.61x - 815.26x^2 - 0.270$. [B] Aqua nadir subgroup, $r^2 = 0.47$ with linear function ($n = 50$; RMSE $= 0.005$; $Fratio_{LUE} = 40.68$; $p \leq 0.000$). Equation: $y = 11.462x - 0.109$. [C] Aqua backscatter subgroup, $r^2 = 0.26$ with linear function ($n = 62$; RMSE $= 0.007$; $Fratio_{LUE} = 22.53$, $p = 0.049$, with significant site differences, $p \leq 0.000$). Equation: $y = 9.168x - 0.058$. With site and site $*$ dailyLUE factors included, $r^2 = 0.56$ (RMSE $= 0.004$ and $Frat_{LUE} = 4.07$, $p \leq 0.05$). [D] Terra forward scatter subgroup, $r^2 = 0.31$ with linear function ($n = 100$; RMSE $= 0.008$; $Fratio_{LUE} = 44.48$, $p < 0.000$, $p \leq 0.000$). Equation: $9.661x - 0.030$. With site and site $*$ dailyLUE factors included, $r^2 = 0.43$ (RMSE $= 0.007$; $Fratio_{LUE} = 37.79$, $p \leq 0.000$). [E] Terra nadir subgroup, $r^2 = 0.37$ with nonlinear function ($n = 68$; RMSE $= 0.006$; $Fratio_{LUE} = 19.61$, $p \leq 0.000$). Equation: $y = 41.96x - 981.09x^2 - 0.271$. [F] Terra backscatter subgroup, $r^2 = 0.39$ with linear function ($n = 86$; RMSE $= 0.006$; $Fratio_{LUE} = 43.27$, $p \leq 0.000$). Equation: $y = 10.67x - 0.06$.

Table 7
PRI(1,11) vs. Daily Tower LUE. Data were analyzed separately for each view observation subset, for each satellite. A simple GLM model was examined for these 3 factors: LUE, site, site ∗ LUE. The bold values show the significant variables (P < 0.05).

		GLM summary statistics					Variables		
Satellite	View subgroup	N	r^2	RMSE	F-ratio$_{LUE}$	Linear equation	LUE	Site	Site ∗ LUE
Terra	Forward	99	0.45	0.007	40.890	$y = -0.074 + 14.99 * LUE$	**0.000**	**0.016**	**0.004**
	Nadir	68	0.34	0.007	6.090	$y = +0.008 + 8.62 * LUE$	**0.016**	0.085	0.089
	Backscatter	86	0.39	0.005	26.300	$y = -0.082 + 12.01 * LUE$	**0.000**	ns	ns
Aqua	Forward (Q)	50	**0.79**	0.003	27.640	$y = -0.296 + 42.56 * LUE - 920.74 * LUE^2$	**0.000**	ns	ns
	Forward (L)	54	**0.75**	0.003	32.940	$y = -0.173 + 19.17 * LUE$	**0.000**	ns	ns
	Nadir	50	0.54	0.005	3.040	$y = -0.044 + 8.25 * LUE$	0.088	ns	ns
	Backscatter	62	0.56	0.004	4.060	$y = +0.022 + 5.23 * LUE$	0.049	**0.019**	**0.021**

(p = 0.088). None of the Terra subsets (F, N, B) performed as well as the comparable Aqua subsets, with r^2 values ranging between 0.34 and 0.45, and RMSEs between 0.005 and 0.007 mol C mol^{-1} absorbed quanta. The lower ability of these simpler models [Table 7], which are only based on LUE as the primary independent variable, to adequately explain the observed MODIS-PRI variability showcases the influence of confounding variables on retrieval success. For example, MODIS-PRI for Terra backscatter views had 21% lower ability to explain LUE in these statistical models than with the full models (r^2, 0.39 vs. 0.60; Tables 7 vs. 5 A]. Equations relating PRI(1,11) to daily LUE are given for the geometry subsets (F, N, B) per satellite in Table 7.

4.10. MODIS-PRI models

We evaluated the relative success of using observed vs. modeled values of LUE. First, we compared our computation of the operational MODIS GPP model (MOD17), referred to here as MOD17LUE, with in situ LUE for the original full dataset (n = 406) (Fig. 7A). There were 14 cases that could not be modeled because of missing meteorological data. We obtained a moderate correlation (r = 0.55; RMSE = 0.007 mol C mol^{-1} absorbed quanta) between the modeled and observed LUE values [Table 8]. Compared with our previous site-corrected results for the full dataset, 35% more scatter occurred in the modeled MOD17LUE compared with the in situ LUE that was directly estimated empirically using the previously introduced variable, PRI-LUE (Fig. 3, Tables 4, 8).

Then, we examined the MOD17LUE vs. the PRI-LUE, limited to the Aqua forward scatter subset using the site-specific regression equations (Table 4, Fig. 3). This comparison of MOD17LUE vs. MODIS-PRI for the Aqua forward subset produced a similar but only slightly better outcome than was obtained for the full dataset (r = 0.57; RMSE = 0.004 mol C mol^{-1} absorbed quanta; F-ratio$_{LUE}$ = 19.04; n = 51). The regression equation was: MOD17LUE = 0.006 + 0.66 ∗ LUE [Table 8, Fig. 7B]. Therefore, we conclude that MOD17LUE was only modestly successful in matching the in situ LUE at the flux towers, whether determined for the full dataset or for the Aqua forward scatter subset. Most importantly, the PRI-LUE computed for the Aqua forward subset *by itself* produced a strong correlation (r = 0.80) with the in situ LUE (RMSE = 0.003; F-ratio$_{LUE}$ = 95.33; n = 54), as shown in Fig. 7C. The general equation describing PRI-LUE in Aqua forward views across sites is: PRI-LUE$_{Aqua,F}$ = 0.008 + 0.420 ∗ (tower LUE) (Approach #1 in Table 8).

This series of analyses demonstrates that the agreement of the satellite-determined MODIS-PRI is strongly affected by the viewing geometry, and that the forward scatter collection from Aqua provided the most consistent data source for tracking in situ LUE at these four study sites during summertime in multiple years.

4.11. Combining same day Terra and Aqua PRIs vs. daily LUE

We examined one more subset of the full dataset, those scenes collected on the same day by Terra (morning) and Aqua (early afternoon), finding 92 "same day" pairs. Several combinations of Terra and Aqua

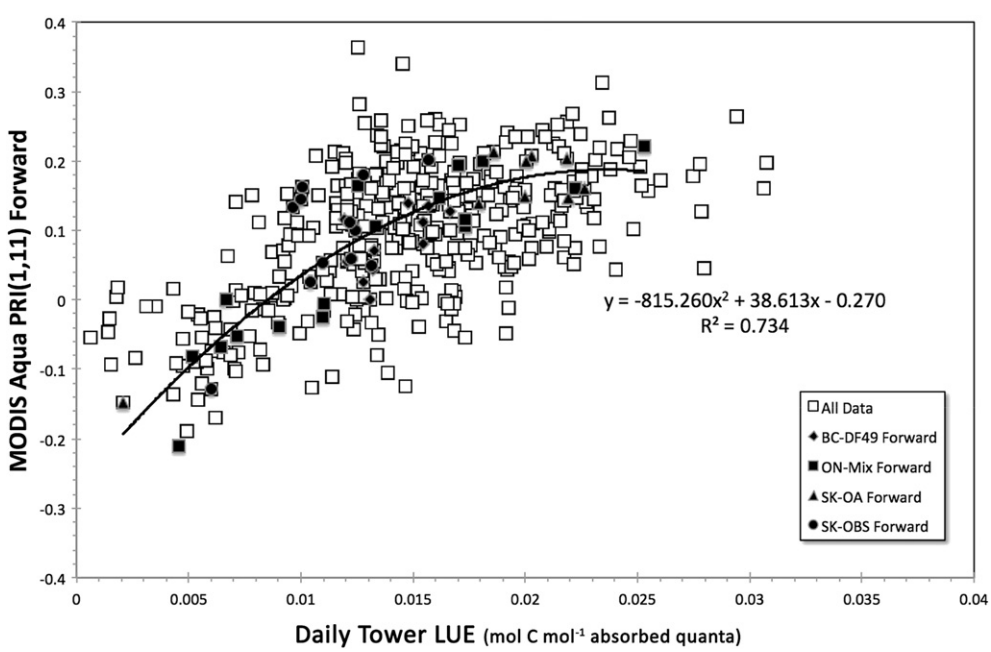

Fig. 6. The Aqua forward scatter observations are overlaid on the full dataset. The Aqua forward views (n = 50, symbols filled) are superimposed on the full dataset (n = 420) and fitted with a power function (see Fig. 5A).

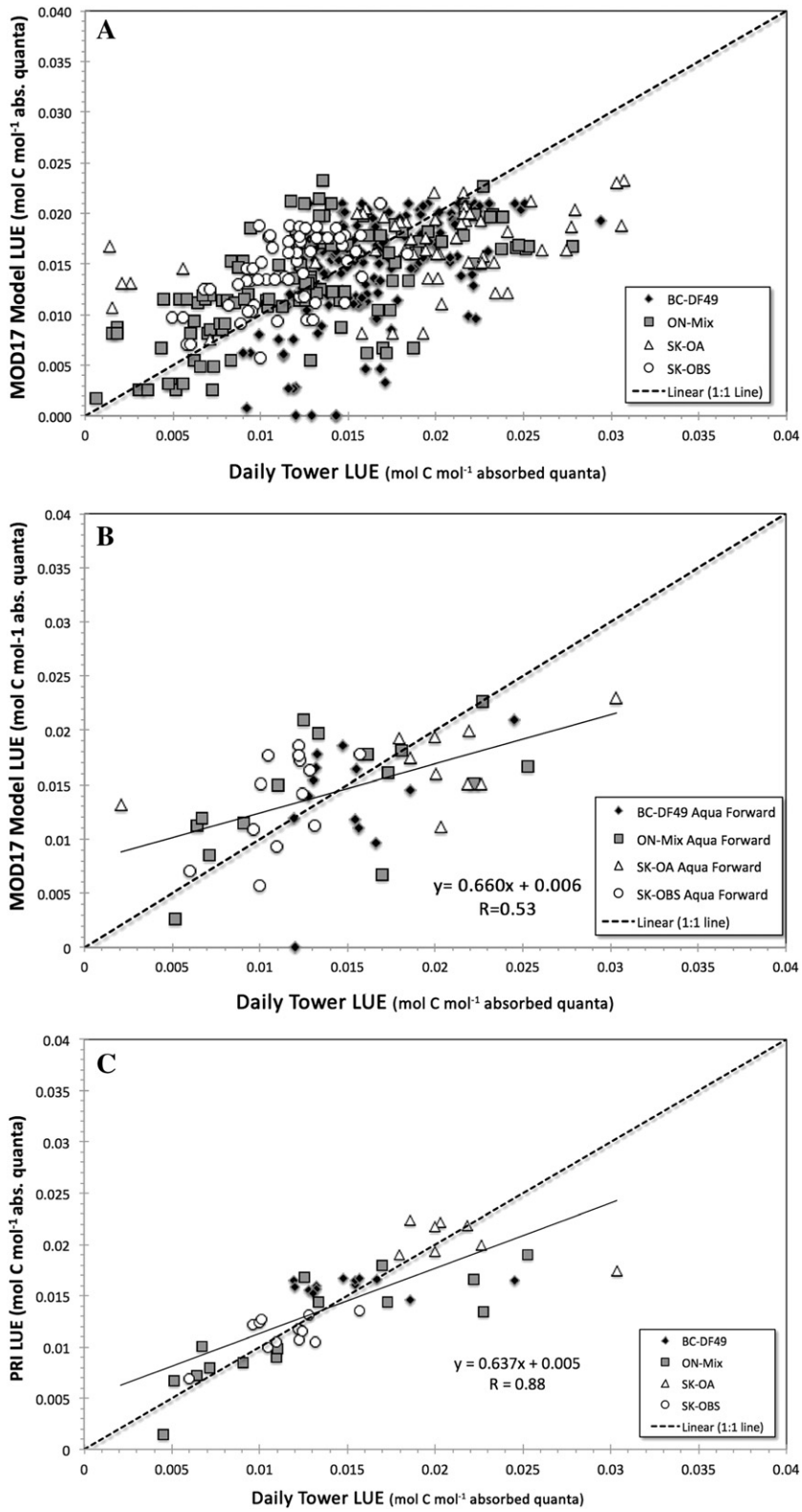

Fig. 7. Modeled LUE vs. daily in situ LUE from flux towers are shown. Symbols represent data from the different sites: black diamonds, BC-DF49; gray squares, ON-Mix; white triangles, SK-OA; and white circles, SK-OBS. The 1:1 lines are shown on each panel (A–C). [A] LUE derived from the MOD17 GPP algorithm vs. observed daily tower LUE. The correlation coefficient relating the MOD17 to observations for all views, $r = 0.55$ ($n = 420$). [B] LUE derived from the MOD17 GPP algorithm vs. observed daily tower LUE, for the subset of the data with Aqua forward views only: $r = 0.53$ ($p < 0.000$, $n = 51$). Equation: $y = 0.452\times + 0.008$. Symbol shapes indicate sites, and dark gray fill indicates that these points are forward views. [C] LUE derived from PRI(1,11) vs. observed daily tower LUE, for the Aqua forward views only: $r = 0.80$ ($p < 0.000$, $n = 54$). Equation: $y = 0.637\times + 0.005$. Adding the site ($p = 0.004$) and site * LUE interaction ($p = 0.044$) factors improved the correlation ($r = 0.88$). Symbol shapes indicate sites, and dark gray fill indicates that these points are forward views.

Table 8
Model approaches for estimating Tower LUE from MODIS data. MOD17 uses the MODIS LUE method. PRI-LUE uses Aqua forward scatter view subgroup. PRI_{sum} uses the sum of same day PRI values from Terra and Aqua. The bold values show high correlation coefficients (r > = 0.7) and highly significant LUE (p < 0.01).

			GLM Summary Statistics					Variables		
	MODELS	Dataset	N	r	RMSE	F-ratio	linear equation	LUE	Site	Site * LUE
MODIS method	MOD17 vs. Tower LUE	Full	420	0.55	0.005		N/A	0.000	ns	N/A
	MOD17 vs. Tower LUE	Aqua forward subset	51	0.59	0.004	19.04	y = 0.006 + 0.660 * LUE	**0.000**	ns	ns
Approach #1	PRI-LUE vs. Tower LUE	Aqua-forward subset	54	**0.80** **0.88**	0.003	20.100	y = 0.008 + 0.420 * LUE	**0.000** **0.000**	0.004	ns 0.044
Approach #2	PRI_{sum} vs. Tower LUE	Same day subset, Terra + Aqua	92	**0.70**	0.013	49.124	$y = -0.216 + 28.489 * LUE_{AV}$	**0.000**	ns	ns

PRI(1,11) values (as the difference, sum, and normalized difference) were compared with the in situ LUE. The PRI_{sum} ($PRI_{Terra} + PRI_{Aqua}$) provided the best agreement with in situ LUE. The variability of PRI_{sum} across sites is displayed as a box plot in Fig. 8A, where SK-OA had the highest PRI_{sum} daily mean and standard error (0.289 ± 0.046); lower but similar values were obtained for the other sites: SK-OBS (0.135 ± 0.042), BC-DF49 (0.127 ± 0.026), and ON-Mix (0.102 ± 0.033). Although these site means were similar, the median values and their ranges were more variable across sites, as shown in the additional boxplots [Fig. 8B].

Three view geometry subgroups comprised most of the 92 Terra-Aqua pairs: forward scattered Terra and backscattered Aqua views, $T_F\_A_B$ (n = 28, average PRI_{sum} = 0.152); backscattered Terra and forward scattered Aqua views, $T_B\_A_F$ (n = 25, average PRI_{sum} = 0.139); and nadir views for both, $T_N\_A_N$ (n = 22, average PRI_{sum} = 0.133). The remaining 17 pairs were associated with nadir views paired with the four possible back or forward views (n = 3, 3, 5, 6). The linear relationship [Fig. 9] of daily PRI_{sum} to daily tower LUE for this combined Terra-Aqua same-day subgroup was moderately strong (r^2 = 0.622; RMSE = 0.013; p ≤ 0.000; F-$ratio_{LUE}$ = 147.91, n = 92). The regression equation was: daily PRI_{sum} = −0.218 + 26.730 * (daily tower LUE). Furthermore, it did not matter which geometry subgroup (F, N, B) was available for pairing the Terra and Aqua MODIS-PRIs in this approach, and there were no other significant site-related factors.

This combined approach was successful because Terra morning MODIS-PRI values were, in general, higher than the early afternoon Aqua MODIS-PRI values. Also, when Aqua MODIS-PRI values remained as high as, or higher than, the earlier same day Terra MODIS-PRI values, daily PRI_{sum} achieved the highest attained values and occurred in conjunction with high in situ daily LUE values [Fig. 9]. On the other hand, when Aqua MODIS-PRI values were lower than those acquired earlier in the same day by Terra due to emergence of stress responses, the daily PRI_{sum} was also lower, and tied to lower in situ daily LUE values.

4.12. Summary of results

This study found that for the full Terra/Aqua collection (2 satellites, 4 sites, all views, all dates), MODIS-PRI computed using green ocean Band 11 and red land Band 1 performed better than other candidate indices, but was still only modestly related (r^2 = 0.33) to in situ daily LUE determined at calibrated flux towers located in our Canadian forest sites (Fig. 2A; Table 5A), when confounding factors were not considered. When site-related regression equations were developed (Fig. 2B; Tables 4 & 5B) and applied to derive a new parameter, PRI-LUE, the variation due to site differences was reduced by 18%, improving the correlation between MODIS-derived predictions and in situ observations (r = 0.72, Fig. 3). Most importantly, the full dataset (n = 420) showed considerable PRI(1,11) variation among the view geometry subgroups per satellite at each site (Fig. 4A,B; Table 5C). When the view geometry subgroups (F, N, B) were explicitly examined separately across the four sites for the two satellites (Fig. 5A–F, Table 6), the most consistent finding was that the Terra nadir and forward scatter PRI(1,11) morning values were significantly higher than those collected in the afternoon by Aqua (Fig. 4B). We then determined that the Aqua forward scatter subgroup provided the most successful approach for describing daily tower LUE (r^2 = 0.75–0.83, Fig. 5; Tables 6 & 7) across the four sites. Nadir views acquired with either Terra or Aqua yielded acceptable daily LUE estimates (r^2 ~ 0.66); however, Aqua nadir values are preferred because they were not affected by other potentially confounding factors (Table 6). Depending on which dataset was examined (full dataset, various subsets), RMSEs for LUE varied between 0.003 and 0.007 mol C mol^{-1} absorbed quanta.

The MOD17LUE estimates were only modestly correlated with daily tower LUE (Table 8) for either the whole dataset (r = 0.55; Fig. 7A) or for the scenes providing the highest performing Aqua forward subgroup (r = 0.59; Fig. 7B). Notably, however, the MODIS-derived PRI-LUE parameter for the Aqua forward subgroup was well correlated to daily tower LUE (r = 0.80; Fig. 7C; Table 8). In addition, by combining same day Terra and Aqua PRI(1,11) values to produce a new variable, PRI_{sum} ($PRI_{Terra} + PRI_{Aqua}$, Fig. 8A,B), a moderately strong relationship emerged to relate a derived MODIS-PRI variable to tower LUE (r^2 = 0.62; Fig. 9). For this last variable, view geometry and site differences were not important but the RMSE (0.013 mol C mol^{-1} absorbed quanta) was four times greater than for the Aqua forward subgroup (0.003 mol C mol^{-1} absorbed quanta). Nevertheless, we demonstrate three different approaches to utilize MODIS-PRI for estimating in situ LUE, based on: (i) Aqua PRI(1,11) forward views, which had the lowest RMSE and no requirement for site regression equations; (ii) the combined same day Terra-Aqua PRIs (PRI_{sum}), also without need for site information, but this option produced the largest RMSE (0.013 mol C mol^{-1} absorbed quanta) associated with the LUE estimate; and (iii) the PRI-LUE variable developed from site-based regressions and applied to either the Aqua forward view subgroup (preferred) or the full dataset (acceptable).

5. Discussion

The results of this study point to the potential development of an operational GPP model that uses LUE derived from MODIS-PRI observations, rather than being simulated from biome-scale look up table values of ε^* and expected vegetation responses to meteorological conditions. This new type of remote sensing driven model would provide an improvement over those existing models, by directly measuring plant responses to daily stresses and seasonal changes. Further, this PRI approach would provide better characterization of GPP or LUE spatial variability across the landscape as demonstrated with regional maps by previous researchers (Drolet et al., 2008; Huemmrich et al., 2013).

Our study demonstrates that accurate retrievals of in situ daily LUE at flux towers can be accomplished from MODIS-PRI measurements during the summertime period associated with maximal photosynthetic activity. In order to accomplish this, the directionality of the views must be considered as well as the timing of the observations in terms of the dynamic diurnal cycle of photosynthesis related physiological processes.

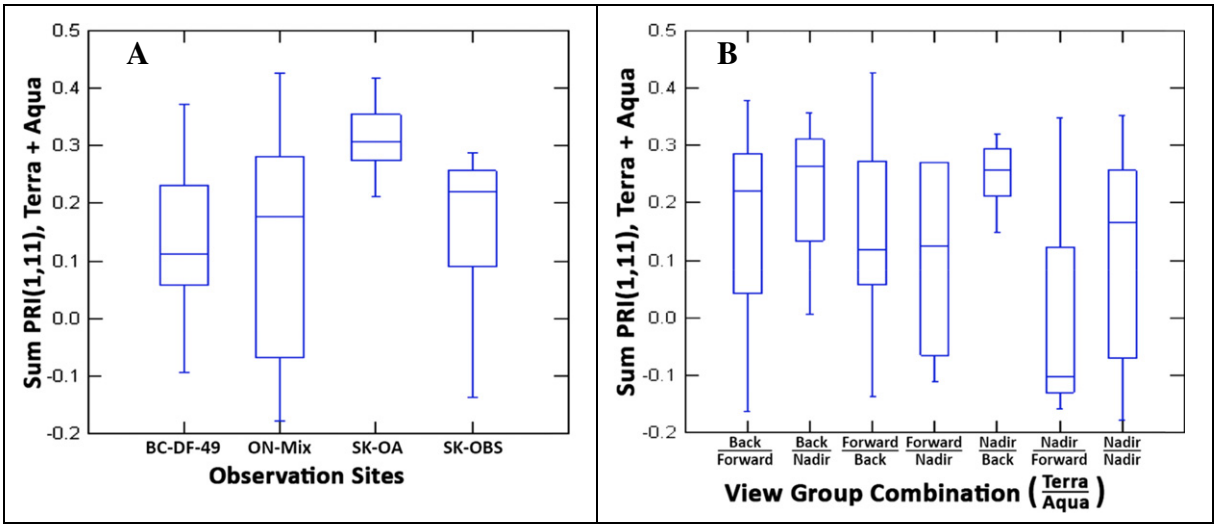

Fig. 8. Box plots for the combined Terra and Aqua PRI(1,11) values for collections made from the two satellites on the same day (n = 92): [A] by Site; and [B] by AM/PM view group combinations, where the view group from Terra is given first, followed by that for Aqua (e.g., B/F, Terra AM collections were made from backscatter views, whereas Aqua PM collections were made from forward views. In box plots, the center horizontal line per group marks the median of the sample, and the box length shows the central 50% range for values.

Our results demonstrate the value of retaining and utilizing off-nadir reflectance information and show that the nadir BRDF-adjusted NBAR method commonly utilized for 8- and 16-day MODIS image composites may not provide the best approach for dynamic vegetation processes such as daily GPP estimates.

Reasons for the better agreement of forward view information as compared to that from backscatter views may be related to the closer azimuth position (by ~8°) of the MODIS forward observations to the SPP (Fig. 1), and because the forward signal benefits from transmission through foliage, thus expressing biochemical information. The possible connection to vegetation function of the relatively higher forward view values associated with vegetation indices (e.g., NDVI; Enhanced Vegetation Index, EVI; PRI) has not been appreciated nor incorporated into the MODIS processing schemes. Even though MODIS PRI observations are not collected along the SPP where maximum/minimum values occur, as was shown in Fig. 1, the geometrical sectors of ecosystems that are viewed can discriminate the edges of forward (cold spot) and backscatter (hotspot) sectors, as shown in Fig. 10. This figure was redrawn from data presented in Cheng et al. (2010), and shows how the PRI changes linearly when viewed sequentially through the full view azimuth angle range for cornfields (VZA = 30°) at three growth stages, expressing mid-day responses related to viewing conditions, phenology,

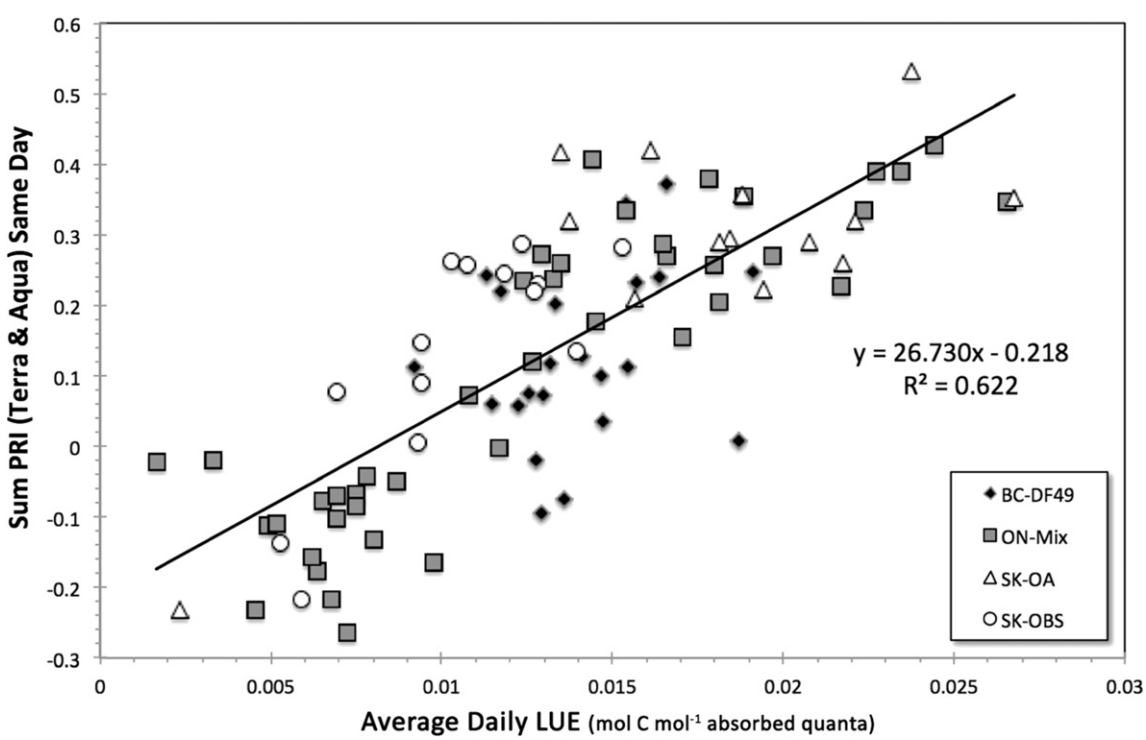

Fig. 9. The daily sum for PRI(1,11) computed from Terra + Aqua across the four study sites (n = 92). The daily average LUE was computed as the average of the two flux tower LUE values determined at the overpass times: $r^2 = 0.622$; RMSE = 0.013; F-ratio, LUE = 147.91; $p < 0.000$). y = 26.73 ∗ LUE - 0.2176. Influences from Site or View group combinations were not significant factors, but identifying the sites reduced the overall unexplained variation by 6% ($r^2 = 0.679$; F-ratio, LUE = 46.53).

and stress levels. The linear decline in the PRI from coldspot to hotspot observed in the cornfield was similar to that observed in the Canadian forests with MODIS.

5.1. New approaches using MODIS-PRI

We present two new approaches for the use of MODIS observations for tracking ecosystem scale LUE. These options rely on either directional MODIS-PRI derived from Aqua's forward views or from combined same day Terra/Aqua "any view" observations. The success of these approaches is a consequence of mid-day physiological stress being expressed that activates the foliage's protective xanthophyll cycle responses in time to be observed with the Aqua overpass, in contrast to lower morning stress conditions observed from Terra in these ecosystems. These approaches appear to be viable in biomes of the northern hemisphere's higher latitudes, where a ~ 2 h interval between Terra and Aqua overpass times corresponds to the local mid-day period when stress responses associated with photosynthetic processes are expressed strongly enough to affect spectral observations made from space. Neither of these remote sensing options require site descriptions (e.g., coniferous vs. deciduous forest) or any meteorological information (temperature, humidity, etc.), so that both approaches are excellent candidates for future operational implementation from space. Either approach opens new possibilities for quantifying ecosystem carbon dynamics.

The first of these successful approaches from this study of four Canadian forests relies on the combined forward scatter view sectors of both Terra and Aqua to provide strong relationships with in situ LUE, although the best retrievals were made solely with Aqua (PM) forward sector MODIS-PRI observations. This is probably because the Aqua overpass coincided with the time of day (early afternoon) when carbon and water exchanges were most impacted by environmental conditions such as higher illumination and temperatures. We suggest that the option exists to track ecosystem LUE by utilizing MODIS-PRI acquired from Aqua if a sufficient number of forward view overpasses are available, or by using forward scatter views from both Aqua and Terra to increase opportunities to observe a given location. The successful demonstration of Aqua data for LUE estimates may provide insurance if Terra becomes unavailable.

The second successful approach leverages the discovery that Terra's morning MODIS-PRI was typically higher than comparable Aqua afternoon MODIS-PRI, especially for forward and nadir views. This finding satisfies our original expectation put forth when we began our initial MODIS-PRI studies (Middleton et al., 2004). A new combined spectral variable, PRI_{sum}, apparently scales linearly with LUE, independent of site type in these forests. This combined data approach takes advantage of two "same day" MODIS-PRI values acquired at critical times in the diurnal photosynthetic dynamical process. We demonstrated that by combining same day Terra + Aqua MODIS-PRI "any view" observations, a reasonable daily LUE estimate per site could be made, although the RMSE error is higher than for the Aqua forward view option (0.013 vs. 0.003 mol C mol^{-1} absorbed quanta). This lower accuracy may be a consequence of the large number of same day Terra/Aqua pairs having nadir views (T_N–A_N), since nadir views were among the lower performing data subsets for estimating LUE. Since the combined same-day PRI_{sum} variable successfully utilized any available Terra/Aqua F, N, B combination, view geometry influences were apparently trumped by diurnal changes. This space-based finding is consistent with many published studies at leaf and canopy levels.

Given the ~2 h mid-day difference between Terra AM and Aqua PM overpass times at the latitudes of our study sites, we now asked whether estimates of in situ LUE determined from instantaneous AM vs. PM observations differed. We found that the half-hourly values of tower LUE at the overpass times for Terra and Aqua for days where both observations were available averaged higher LUE at the Terra overpass time compared with Aqua (Figure 11). Therefore, we re-examined those days that had both Terra and Aqua acquisitions, comparing the two estimates of half-hourly tower LUE available from the same day. This revealed that Aqua-based half-hourly LUE estimates had a somewhat higher correlation (r = 0.94) than those based on Terra (r = 0.89), demonstrating that the time of overpass may be an important factor in the performance of Aqua versus Terra observations for daily LUE estimates. This also gives further credence to our explanation that those stress conditions expressed in the early afternoon periods, and which are observed

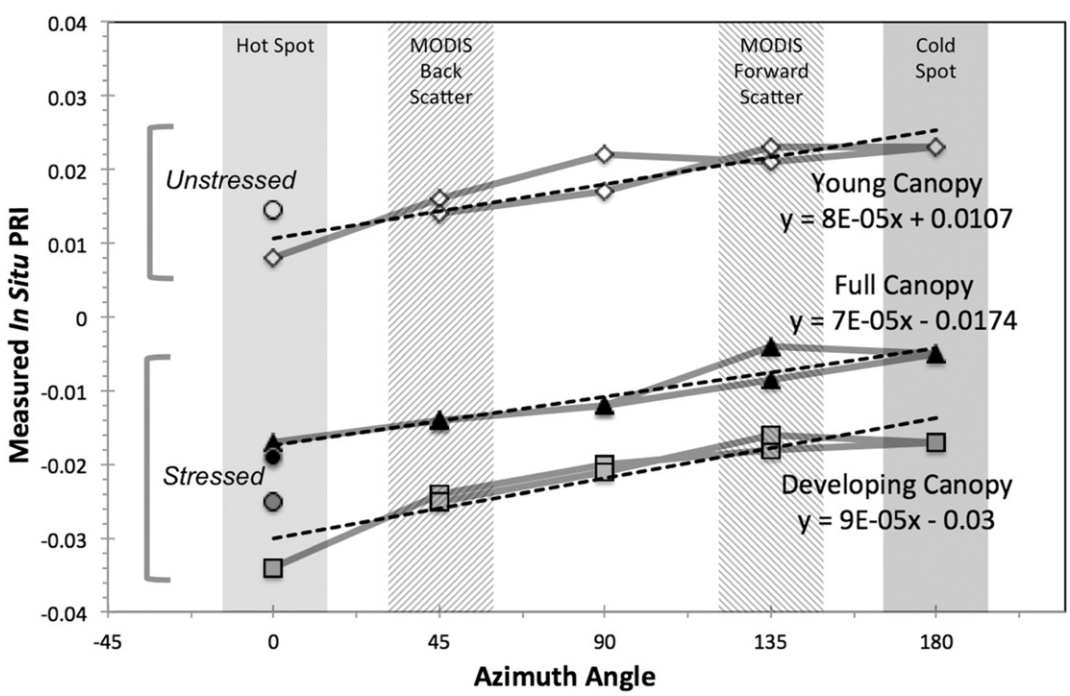

Fig. 10. Corn PRI as measured in the BARC OPE3 cornfield at View Zenith Angle of 30°. The PRI was computed from 531 and 510 nm. Young Canopy (white diamond), y = 0.00008× + 0.0107; Developing Canopy (gray square), y = 0.00009x − 0.03; Full Canopy (black triangle), y = 0.00007x − 0.0174. Note the closeness of the slopes of the various regression lines. The circular points (at 0° Azimuth angle) are the nadir measurements (on the plot for reference). (Fig. adapted from Cheng et al., 2010).

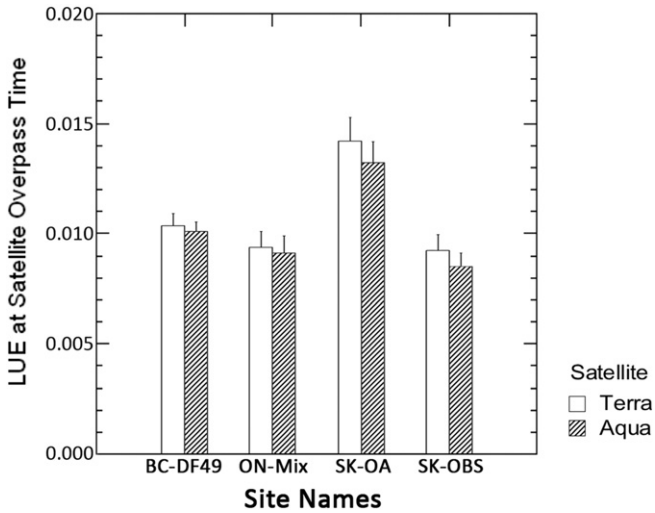

Fig. 11. For the analysis of same day satellite pairs, when both Terra and Aqua viewed the sites, the morning LUE (Terra overpass time) determined at the flux towers was always higher than the afternoon LUE (Aqua overpass time), for data averaged over collections made throughout the growing season and from different years.

with Aqua MODIS-PRI, allow greater differentiation among sites, and further, that the less stressed morning conditions may make sites appear more similar when observed from Terra. Although differences in Terra vs. Aqua instrument responses have been observed (Franz et al., 2008), we did not detect differences attributable to instrument responses.

A third approach for LUE estimation from PRI was demonstrated in this study, based on a second new variable, PRI-LUE, which correlated strongly with observed ecosystem LUE. This empirical approach relies on development of site-specific MODIS-PRI vs. LUE regression equations. This direct remote sensing approach for estimating LUE from MODIS-PRI was superior to the MOD17 modeling approach, which defines maximum LUE (ε^*) at the biome rather than the ecosystem level and requires meteorological data inputs for these sites. We also mention that other direct remote sensing approaches based on multiband full spectrum information are also proving successful for LUE estimation from space using MODIS data (Zhang et al., 2009; Cheng et al., 2014; Zhang et al., 2016).

The correlation of MOD17LUE to daily tower LUE was only moderate ($r = 0.59$), whereas a much stronger correlation was achieved between the PRI-LUE and daily tower LUE ($r = 0.80$), when the site-specific relationships were included (e.g., differences in slopes) to distinguish coniferous from deciduous forests. Although not suitable for general operational implementation because of the need for site-specific equations, we recommend this approach for time series at remote sensing validation sites stationed at flux towers to support remote sensing monitoring programs.

5.2. Confounding factors

We found that a number of factors conspire to confound usage of a simple model describing MODIS-PRI as a function of LUE. Our study corroborates earlier studies that find that MODIS-PRI retrievals of in situ LUE are sensitive to many factors, which vary among sites and environmental conditions. These poorly described sources of variation explain, in part, why some studies are successful and others are not in using MODIS-PRI for stress detection. We show that several variables describing various aspects of differing/changing illumination and geometry conditions had significant influences on the MODIS-PRI vs. LUE relationships, in addition to site- and satellite-related differences. Sorting out the influence of all of these potentially confounding factors requires thorough statistical evaluation to quantify their contributions. However, we note that our study had uneven and unequal group sample sizes per site, satellite, and view group, which influences the statistical analyses.

We show that seasonality within the summertime period examined and year to year differences actually did contribute to variations in the observed PRI(1,11) values, and may have been associated with factors such as water availability/deficits and plant pigment changes (e.g., chl:carotenoid ratios) over time. We found that the spectral pigment index for carotenoid content (CRI) was marginally significant ($p \leq 0.09$) for only two data groups (full dataset, SK-OBS). The inclusion of this spectral index was an exploratory exercise, given that the published equation could not be perfectly matched with MODIS bands. If an Earth-looking spectrometer (e.g., EO-1/Hyperion) had been tasked to provide repetitive observations at our study sites, we could have duplicated the published wavelengths in the computation of this and other pigment indices.

One of the geometry variables identified as an important parameter affecting the PRI, SZA, was not found to contribute significantly to explaining the PRI relationship to LUE in our study. The reasons for this are that: (i) the study deliberately only examined the green-up period when the MODIS NBAR NDVI was stable at each of the four sites, in multiple years; (ii) the influence of the other illumination-related and/or phenology-related variables (PAR, fAPAR, DOY, Year) cannot be independently separated from the seasonal SZA changes; and (iii) the study examines satellite observations collected during the middle period of the day (~10 am–3 pm) when SZA is highest and is relatively similar for a late morning (Terra) and an early afternoon (Aqua) collection. The one exception is the Old Black Spruce site where SZA and tower LUE provide the same influence on the MODIS PRI, causing only one of them to produce a significant result, possibly due to shadowing effects at that more open site. In the view angle subsets, the inclusion of the SZA as an analysis variable did not help us understand the behavior of the MODIS PRI relationship to LUE.

5.3. Limitations in the use of MODIS-PRI for LUE

There are some important limitations to the use of MODIS-PRI data for LUE retrieval via space-based measurements. An important confounding factor is that MODIS observations are not acquired in the SPP, falling between the instantaneous SPP and its perpendicular cross-plane. This azimuth offset varies according to time of day, time of year and latitude. Since MODIS observations do not line up with the SPP, the optimal signal to observe PRI differences between shaded (cold spot) and illuminated (hotspot) foliage (Hilker et al., 2008; Middleton et al., 2009a, 2014; Cheng et al., 2009, 2010) is not possible to achieve with Terra or Aqua. However, the differences between hotspot and cold spot PRI values are still distinguishable in the overlap areas near the azimuth cross-plane as reported by Middleton et al. (2009a) and Cheng et al. (2010) for corn canopies. In this overlap area, the MODIS fields-of-view contain mixtures of shadowed and illuminated foliage. This issue requires further study as it represents a potential trade-off between increasing the number and temporal resolution of observations against inherent signal discrimination limits in the determination of LUE from MODIS-PRI in non-optimal viewing sectors.

Another important limiting factor to the use of MODIS-PRI for LUE ecosystem estimations is that the ocean bands have much coarser 1-km resolution than is desired for many terrestrial ecosystem studies. And, the desired reference band at 570 nm is not included in the MODIS suite. We chose to use Band 1 (the 50 nm wide red land band, at 250 m resolution) as the reference band instead of one of the two red ocean bands, because it has less noise due to a wider band-width, and can be scaled up to a 1-km field of view. However, the choice of best reference band is not clear-cut and has implications for the interpretation of the MODIS-PRI computed. The traditional PRI with a reference band at 570 nm provides a range of values that the community can interpret in terms of relative stress status. Since the MODIS PRI(12,11) computed in this study was too noisy for use, such that a transfer function could not be achieved between these two PRI versions, we do not

have the necessary information to determine the equivalent value ranges that are associated with stress/non-stress in this or the alternative MODIS-PRI variations that we examined. We also note that what we refer to as PRI(1,11) is similar to the Carotenoid Chlorophyll Index (CCI) defined by Wong and Gamon (2015a) and Gamon et al. (2016), which has a reference wavelength of 620 nm (vs. MODIS B1, 645 ± 25 nm), which they conclude varies seasonally with changing leaf chlorophyll and carotenoid pool sizes.

Studies applying MODIS-PRI at sites with limited variation in LUE may not be able to find a significant relationship because the inherent noise in the MODIS-PRI may overwhelm the signal as, for example, in the Douglas fir site in this study. However, within the limitations of using the data processing approach for ocean bands over land, in a similar manner used for the MODIS land bands with single images (rather than temporal composites), the MODIS-based LUE measurements provided a more accurate estimation of observed LUE than the values presently derived in the MODIS GPP model, which requires meteorological data. Further, improved methods for processing of MODIS data to surface reflectance have been shown to provide more accurate values of PRI (Hilker et al., 2009; Zhang et al., 2016). Application of improved calculations of MODIS surface reflectance (e.g., Lyapustin et al., 2011) may reduce the noise in the MODIS PRI-LUE relationships.

Frequent temporal intervals are also important to capture the carbon dynamics at ecosystem scales. The best strategy for image collections for LUE retrievals, whether accomplished with forward scatter views or with same day Terra/Aqua collections, should aim to reduce the time intervals between satellite day-to-day observations and consequently provide a more dense time series. This is important because even during periods with stable green LAI, GPP can change dramatically. For example, within a single week during 2004, in situ daily GPP at ON-Mix spiked from 0.52 to 0.82 (the corresponding LUE variability changed from near 0 to over 0.03 mol C mol^{-1} absorbed quanta) before stabilizing at an intermediate value of 0.66 mol C m^{-2} day^{-1}. Thus, during the critical mid-summer period, MODIS-PRI can potentially provide important information for determining GPP of forests when frequent observations can be obtained.

5.4. Next generation satellites

Unfortunately, most multi-spectral Earth Observing satellite sensors such as the Landsat series do not have the physiologically necessary PRI band centered at 530 nm, and/or they lack the reference band at 570 nm as is the case for MODIS. And, with the aging of the Terra and Aqua satellites, the timeframe is limited for ongoing utilization of MODIS-PRI. Regrettably, the Visible Infrared Imaging Radiometer Suite (VIIRS) instrument flying on the Suomi National Polar-orbiting Partnership (NPP) satellite, intended to be the continuation of MODIS, did not retain the critical 531 nm band needed for calculation of PRI. However, there are two NASA satellite concepts under development that could rectify this omission and enable future PRI time series. The first is the Pre-Aerosol, Cloud, ocean Ecosystem (PACE) mission (with a proposed 1-km spatial resolution and launch targeted for 2022) that will have a high spectral resolution imaging spectrometer (Del Castillo and Platnick, 2012). PACE offers the possibility to continue the PRI time series for terrestrial ecosystems, including nadir/off-nadir observing views, even though its primary purpose, like Aqua, is to observe ocean surfaces. Another opportunity for PRI estimates of LUE will be available at a spatial resolution (≤60 m) relevant for terrestrial ecosystems from the Hyperspectral Infrared Imager (HyspIRI) (Lee et al., 2015), but with much less frequent twice monthly temporal coverage, and with only nadir views. However, HyspIRI has not been yet been selected for Phase A development, and its earliest launch date would be in early/mid 2020s. PRI is now available with ESA's operational multi-spectral Sentinel-3 (launched, Feb 16, 2016) and will be available with global imaging spectrometer missions such as the Fluorescence Explorer's (FLEX) FLORIS sensor, with launch in 2022 to fly in tandem with a Sentinel-3 satellite (Drusch et al., 2016), and with Germany's EnMAP (Gaunter et al., 2015) to be launched in 2018 with potential for drought stress detection with PRI (Dotzler et al., 2015). Most of these missions will have AM overpass times, thereby missing the optimal early PM local times for best stress detection related to LUE and GPP, and non-optimal but acceptable nadir observing views.

Our study highlights the benefit of additional observations on the same day for sites of interest for quantifying dynamic physiological responses that affect the local carbon, water, and energy fluxes. We demonstrate the potential benefit of coordinated space-based spectral measurements, which hints at future possibilities of data fusion techniques. Certainly, merging together these additional information sources would reduce the errors associated with model outputs that rely on parameterization of critical input variables tuned with remote sensing observations. We also highlight the importance of off-nadir directional observations, both in terms of interpreting the signals routinely acquired from space in wide-swath satellite sensors such as MODIS and for designing future satellite sensors to exploit this new understanding. In addition, we note the benefit of combining PRI with solar-induced fluorescence to estimate GPP, as successfully shown for a cornfield over multiple years (Cheng et al., 2013), and recently reported for two agricultural crops (Schickling et al., 2016). More studies that examine these two indices together are needed.

Our study should be repeated in other biomes using MODIS Aqua and Terra data. Airborne campaigns supporting similar twice-daily (mid-morning, mid-afternoon) acquisitions would advance our understanding of these physiological processes at the ecosystem scale. And we strongly recommend the development of space-based visible through shortwave infrared spectrometers to study ecosystem stress responses that capture photosynthetic down-regulation. The ability to make direct LUE determinations from space with the PRI during the peak summertime activity periods that dominate the annual estimates used in carbon models should be a national priority.

6. Conclusion

We provide a rigorous statistical study that identifies the sources of factors that contribute to variations in MODIS-PRI observations, and which can provide a deeper understanding of the reasons for the range of success reported in estimating ecosystem LUE in published studies. Although not designed for this purpose, the narrow green MODIS ocean band centered at 531 nm can be used with a red land band as a reference (MODIS Bands 11 and 1, respectively) to calculate a version of the PRI over forests that is related to ecosystem in situ LUE measured by flux towers. However, use of MODIS-PRI is strongly influenced by viewing geometry factors, such as the view direction and azimuth, and time of day. We show that forward scatter views are the most strongly related to in situ daily LUE, as compared to nadir or backscatter views, especially those forward view observations collected in the early afternoon by Aqua, since significant diurnal differences were apparent in comparing MODIS-PRI values obtained from Terra (AM) and Aqua (PM). We answered all of the questions posed in the Introduction in the affirmative: differences in illumination conditions drive MODIS-PRI variations; differences due to directional geometry of observations affect MODIS-PRI values; Terra (AM) and Aqua (PM) capture different MODIS-PRI values due to expression of diurnal stress responses; and PRI-LUE relationships differed among our four Canadian sites.

Our study offers three new strategies for using MODIS satellite imagery to monitor daily in situ LUE using MODIS-PRI. The first two strategies could enable regional mapping of LUE/GPP and utilize: (i) forward scatter observations only, acquired by either Terra and Aqua; or (ii) “same day” Terra and Aqua pairs, combining PRI observations for any view observations (backscatter, nadir, forward scatter). A third approach requires site-specific regression equations using all available observations, pertinent for use at specific validation sites. All

of these approaches to spectrally retrieve canopy LUE and GPP should be examined for additional ecosystems worldwide, with attention to the benefit to be gained by combining responses obtained at variable Terra-Aqua temporal AM-PM overpass difference intervals across a latitudinal gradient.

Acknowledgments

We would like to thank Dr. Forrest G. Hall (UMBC) for his advocacy of multi-angle reflectance observations of ecosystems. We would also like to acknowledge the research on PRI conducted by Dr. Thomas Hilker (Oregon State Univ., in memorium). Our research was supported by NASA funding on Carbon Cycle Science and the Science of Terra & Aqua. Thanks also to Fluxnet Canada and the Canadian Carbon Program which was supported by the Canadian Foundation for Climate and Atmospheric Science (CFCAS), the Natural Sciences and Engineering Research Council (NSERC) of Canada, and BIOCAP Canada. Additional support was from Environment Canada and Natural Resources Canada.

References

Alton, P.B., 2016. The sensitivity of models of gross primary productivity to meteorological and leaf area forcing: A comparison between a Penman–Monteith ecophysiological approach and the MODIS Light-Use Efficiency algorithm. Agric. For. Meteorol. 218–219, 11–24.

Amiro, B.D., Barr, A.G., Black, T.A., Iwashita, H., Kljun, N., McCaughey, J.H., Morgenstern, K., Murayama, S., Nesic, Z., Orchansky, A.L., Saigusa, N., 2006. Carbon, energy and water fluxes at mature and disturbed forest sites, Saskatchewan, Canada. Agric. For. Meteorol. 136, 237–251.

Asner, G.P., Nepstad, D., Cardinot, G., Ray, D., 2004. Drought stress and carbon uptake in an Amazon forest measured with spaceborne imaging spectroscopy. United States of America]–>Proc. Natl. Acad. Sci. U. S. A. 101 (16), 6039–6044.

Atherton, J., Nichol, C.J., Porcar-Castell, A., 2016. Using spectral chlorophyll fluorescence and the photochemical reflectance index to predict physiological dynamics. Remote Sens. Environ. 176, 17–30.

Baker, I.T., Prihodko, L., Denning, A.S., Goulden, M., Miller, S., da Rocha, H.R., 2008. Seasonal drought stress in the Amazon: reconciling models and observations. J. Geophys. Res. 113 (G00B011). http://dx.doi.org/10.1029/2007JG000644.

Barr, A.G., Black, T.A., Hogg, E.H., Kljun, N., Morgenstern, K., Nesic, Z., 2004. Inter-annual variability in the leaf area index of a boreal aspen-hazelnut forest in relation to net ecosystem production. Agric. For. Meteorol. 126, 237–255.

Barton, C.V.M., North, P.R.J., 2001. Remote sensing of canopy light use efficiency using the photochemical reflectance index: Model and sensitivity analysis. Remote Sens. Environ. 78, 264–273.

Black, T.A., den Hartog, G., Neumann, H.H., Blanken, P.D., Yang, P.C., Russell, C., Nesic, Z., Lee, X., Chen, S.G., Staebler, R., Novak, M.D., 1996. Annual cycles of water vapour and carbon dioxide fluxes in and above a boreal aspen forest. Glob. Chang. Biol. 2 (3), 219–229.

Campbell, P.K.E., Middleton, E.M., Thome, K.J., Kokaly, R., Huemmrich, K.F., Lagomasino, D., Novick, K.A., Brunsell, N.A., 2013. EO-1 hyperion reflectance time series at calibration and validation sites: stability and sensitivity to seasonal dynamics. IEEE J. Selected Topics in Applied Earth Observations and Remote Sensing (JSTARS) 6 (2), 276–290.

Chapin III, F.S., et al., 2006. Reconciling carbon-cycle concepts, terminology, and methods. Ecosystems 9, 1041–1050.

Chen, J., Rich, P.M., Gower, S.T., Norman, J.M., Plummer, S., 1997. Leaf area index of boreal forests: theory, techniques, and measurements. J. Geophys. Res. 102 (29), 429–29,443.

Chen, J.M., Govind, A., Sonnentag, O., Zhang, Y., Barr, A., Amiro, B., 2006. Leaf area index measurements at Fluxnet-Canada forest sites. Agric. For. Meteorol. 140, 257–268.

Cheng, Y.-B., Middleton, E.M., Hilker, T., Coops, N.C., Black, T.A., Krishnan, P., 2009. Dynamics of spectral bio-indicators and their correlations with light use efficiency using directional observations at a Douglas-fir forest. Meas. Sci. Technol. 20 (095107), 15.

Cheng, Y.-B., Middleton, E.M., Huemmrich, K.F., Zhang, Q., Campbell, P.K.E., Corp, L.A., Russ, A.L., Kustas, W.P., 2010. Utilizing *in situ* directional hyperspectral measurements to validate bio-indicator simulations for a corn crop canopy. Eco. Inform. 5, 330–338.

Cheng, Y.-B., Middleton, E.M., Zhang, Q., Huemmrich, K.F., Campbell, P.K., Corp, L.A., Cook, B.D., Kustas, W.P., Daughtry, C.S., 2013. Solar induced fluorescence and the photochemical reflectance index for estimating gross primary production in a cornfield. Remote Sens. 5 (12), 6857–6879.

Cheng, Y.-B., Zhang, Q., Lyapustin, A.I., Wang, Y., Middleton, E.M., 2014. Impacts of light use efficiency and fPAR parameterization on gross primary production modeling. Agric. For. Meteorol. 189–190, 187–197.

Coops, N.C., Hilker, T., Hall, F.G., Nichol, C.J., Drolet, G.G., 2010. Estimation of light-use efficiency of terrestrial ecosystems from space: a status report. Bioscience 60 (10), 788–797.

Coursolle, C., Margolis, H.A., Barr, A.G., Black, T.A., Amiro, B.D., McCaughey, J.H., Flanagan, L.B., Lafleur, P.M., Roulet, N.T., Bourque, C.P.-A., Arain, M.A., Wofsy, S.C., Dunn, A., Morgenstern, K., Orchansky, A.L., Bernier, P.Y., Chen, J.M., Kidston, J., Saigusa, N., Hedstrom, N., 2006. Late-summer carbon fluxes from Canadian forests and peatlands along an east–west continental transect. Can. J. For. Res. 36, 783–800.

Damm, A., Guanter, L., Verhoef, W., Schläpfer, D., Garbari, S., Schaepman, M.E., 2015. Impact of varying irradiance on vegetation indices and chlorophyll fluorescence derived from spectroscopy data. Remote Sens. Environ. 156, 202–215.

Del Castillo, C., Platnick, S., 2012. Pre-Aerosol, Clouds, and ocean Ecosystem (PACE) mission science definition team report (Oct. 16, 2012). Chairs 274.

Dotzler, S., Hill, J., Henning, B., Stoffels, J., 2015. The potential of EnMAP and Sentinel-2 for detecting drought stress phenomena in deciduous forest communities. Remote Sens. 7 (10):14227–14258. http://dx.doi.org/10.3390/rs71014227.

Drolet, G.G., Huemmrich, K.F., Hall, F.G., Middleton, E.M., Black, T.A., Barr, A.G., Margolis, H.A., 2005. A MODIS-derived Photochemical Reflectance Index to detect inter-annual variations in the photosynthetic light-use efficiency of a boreal deciduous forest. Remote Sens. Environ. 98, 212–224.

Drolet, G.G., Middleton, E.M., Huemmrich, K.F., Hall, F.G., Amiro, B.D., Barr, A.G., Black, T.A., McCaughey, J.H., Margolis, H.A., 2008. Regional mapping of gross light-use efficiency using MODIS spectral indices. Remote Sens. Environ. 12, 3064–3078.

Drusch, M., Moreno, J., del Bello, U., Franco, R., Goulas, Y., Huth, A., Kraft, S., Middleton, E., Miglietta, F., Mohammad, G., Nedbal, L., Rascher, U., Schuttemeyer, D., Verhoef, W., 2016. The Fluorescence EXplorer (FLEX) mission concept – ESA's Earth Explorer 8 (EE8). IEEE Trans. Geosci. Remote Sens. (submitted 2/22/2016).

Fensholt, R., Sandholt, I., Proud, S.R., Stisen, S., Rasmussen, M.O., 2010. Assessment of MODIS sun-sensor geometry variations effect on observed NDVI using MSG SEVIRI geostationary data. Int. J. Remote Sens. 31 (23), 6163–6187.

Filella, I., Amaro, T., Araua, J.L., Peñuelas, J., 1996. Relationship between photosynthetic radiation-use efficiency of barley canopies and the photochemical reflectance index (PRI). Physiol. Plant. 96, 211–216.

Filella, I., Porcar-Castell, A., Munné-Bosch, S., Bäck, J., Garbulsky, M.G., Peñuelas, J., 2009. PRI assessment of long-term changes in carotenoids/chlorophyll ratio and short-term changes in de-epoxidation state of the xanthophyll cycle. Int. J. Remote Sens. 30, 4443–4455.

Franz, B.A., Kwiakowska, E.J., Meister, G., McClain, C.R., 2008. Moderate resolution imaging spectroradiometer on Terra: limitations for ocean color applications. J. Appl. Remote. Sens. 2, 023525.

Gamon, J.A., Berry, J., 2012. Facultative and constitutive pigment effects on the Photochemical Reflectance Index (PRI) in sun and shade conifer needles. Israel Journal of Plant Sciences 60, 85–95.

Gamon, J.A., Qiu, H.-L., 1999. Ecological applications of remote sensing at multiple scales. In: Pugnaire, F.I., Valladares, F. (Eds.), Handbook of Functional Plant Ecology. Marcel Dekker, Inc., New York, pp. 805–846.

Gamon, J.A., Peñuelas, J., Field, C.B., 1992. A narrow-wavelength spectral index that tracks diurnal changes in photosynthetic efficiency. Remote Sens. Environ. 41, 35–44.

Gamon, J.A., Serrano, L., Surfus, J.S., 1997. The photochemical reflectance index: an optical indicator of photosynthetic radiation use efficiency across species, functional types, and nutrient levels. Oecologia 112, 492–501.

Gamon, J.A., Field, C.B., Fredeen, A.L., Thayer, S., 2001. Assessing photosynthetic downregulation in sunflower stands with an optically-based model. Photosynth. Res. 67, 113–125.

Gamon, J.A., Huemmrich, K.F., Wong, C.Y.S., Ensminger, I., Garrity, S., Hollinger, D.Y., Noormets, A., Peñuelas, J., 2016. A remotely sensed pigment index reveals photosynthetic phenology in evergreen conifers. Nat. Commun. (in review March 2016).

Garbulsky, M.F., Peñuelas, J., Gamon, J., Inoue, Y., Filella, I., 2011. The photochemical reflectance index (PRI) and the remote sensing of leaf, canopy and ecosystem radiation use efficiencies: a review and meta-analysis. Remote Sens. Environ. 115 (2), 281–297.

Garrity, S.R., Eitel, J.U.H., Vierling, L.A., 2011. Disentangling the relationships between plant pigments and the photochemical reflectance index reveals a new approach for remote estimation of carotenoid content. Remote Sens. Environ. 115, 628–635.

Gaunter, L., Kaufmann, H., Segl, K., Foerster, S., Rogass, C., Chabrillat, S., et al., 2015. The EnMAP spaceborne imaging spectroscopy mission for Earth observations. Remote Sens. 7 (7):8830–8857. http://dx.doi.org/10.3390/rs70708830.

Gitelson, A.A., Gamon, J.A., 2015. The need for a common basis for defining light-use efficiency: Implications for productivity estimation. Remote Sens. Environ. 156, 196–201.

Gitelson, A.A., Zur, Y., Chivkunova, O.B., Merzlyak, M.N., 2002. Assessing carotenoid content in plant leaves with reflectance spectroscopy. Photochem. Photobiol. 75, 272–281.

Goerner, A., Reichstein, M., Rambal, S., 2009. Tracking seasonal drought effects on ecosystem light use efficiency with satellite-based PRI in a Mediterranean forest. Remote Sens. Environ. 113 (5), 1101–1111.

Goerner, A., Reichstein, M., Tomelleri, E., Hanan, N., Rambal, S., Papale, D., Dragoni, D., Schmullius, C., 2011. Remote sensing of ecosystem light use efficiency with MODIS-based PRI. Biogeosciences 8, 189–202.

Grace, J., Nichol, C., Disney, M., Lewis, P., Quaife, T., Bowyer, P., 2007. Can we measure terrestrial photosynthesis from space directly, using spectral reflectance and fluorescence? Glob. Chang. Biol. 13:1484–1497. http://dx.doi.org/10.1111/j.1365-2486.2007.01352.

Guarini, R., Nichol, C., Clement, R., Loizzo, R., Grace, J., Borghetti, M., 2014. The utility of MODIS-sPRI for investigating the photosynthetic light-use efficiency in a Mediterranean deciduous forest. Int. J. Remote Sens. 35 (16), 6157–6172.

Hall, F.G., Hilker, T., Coops, N.C., Lyapustin, A., Huemmrich, K.F., Middleton, E., Margolis, H., Drolet, G., Black, T.A., 2008. Multi-angle remote sensing of forest light use efficiency by observing PRI variation with canopy shadow fraction. Remote Sens. Environ. 112, 3201–3211.

Heinsch, F.A., Reeves, M.C., Votava, P., Kang, S., Milesi, C., Zhao, M., Glassy, J., Jolly, W.M., Loehman, R., Bowker, C.F., Kimball, J.S., Nemani, R.R., Running, S.W., 2003. User's guide: GPP and NPP (MOD17A2/A3) products. NASA MODIS Land Algorithm. Version 1.3. http://www.ntsg.umt.edu/modis/MOD17UsersGuide.pdf

Hilker, T., Coops, N.C., Hall, F.G., Black, T.A., Chen, B., Krishnan, P., Wulder, M.A., Sellers, P.J., Middleton, E.M., Huemmrich, K.F., 2008. A modeling approach for up-scaling gross ecosystem production to the landscape scale using remote sensing data. J. Geophys. Res. Biogeosci. 113 (G3) (Art. No. G03006.).

Hilker, T., Lyapustin, A., Hall, F.G., Wang, Y., Coops, N.C., Drolet, G., Black, T.A., 2009. An assessment of photosynthetic light use efficiency from space: Modeling the atmospheric and directional impacts on PRI reflectance. Remote Sens. Environ. 113 (11), 2463–2475.

Hilker, T., Coops, N., Hall, F., Nichol, C., Lyapustin, A., Black, T., Wulder, M., Leuning, R., Barr, A., Hollinger, D., Munger, B., Tucker, C., 2011. Inferring terrestrial photosynthetic light use efficiency of temperate ecosystems from space. J. Geophys. Res. Biogeosci. 116: 668–675. http://dx.doi.org/10.1029/2011JG001692.

Hipps, L.E., Asrar, G., Kanemasu, E., 1983. Assessing the interception of photosynthetically active radiation in winter wheat. Agric. For. Meteorol. 28, 253–259.

Holben, B.N., 1986. Characteristics of maximum-value composite images for temporal AVHRR data. Int. J. Remote Sens. 7, 1435–1445.

Huemmrich, K.F., Gamon, J., Tweedie, C., Campbell, P.K., Landis, D., Middleton, E., 2013. Arctic tundra vegetation functional types based on photosynthetic physiology and optical properties. IEEE J. of Selected Topics in Applied Earth Observations and Remote Sensing (JSTARS) 6 (2), 265–275.

Huete, A., Didan, K., Miura, T., Rodriguez, E.P., Gao, X., Ferreira, L.G., 2002. Overview of the radiometric and biophysical performance of the MODIS vegetation indices. Remote Sens. Environ. 83 (1), 195–213.

Humphreys, E.R., Black, T.A., Morgenstern, K., Cai, T.B., Drewitt, G.B., Nesic, Z., Trofymow, J.A., 2006. Carbon dioxide fluxes in coastal Douglas-fir stands at different stages of development after clearcut harvesting. Agric. For. Meteorol. 140, 6–22.

Jarvis, P.G., Massheder, J.M., Hale, S.E., Moncrieff, J.G., Rayment, M., Scott, S.L., 1997. Seasonal variation of carbon dioxide, water vapour and energy exchanges of a boreal black spruce forest. J. Geophys. Res. 102 (D24), 28,953–28,966.

Jenkins, J., Richardson, A.D., Braswell, B.H., Ollinger, S.V., Hollinger, D.Y., Smith, M.-L., 2007. Refining light-use efficiency calculations for a deciduous forest canopy using simultaneous tower-based carbon flux and radiometric measurements. Agric. For. Meteorol. 143, 64–79.

Kucharik, C.J., Twine, T.E., 2007. Residue, respiration, and residuals: Evaluation of a dynamic agroecosystem model using eddy flux measurements and biometric data. Agric. For. Meteorol. 146:134–158. http://dx.doi.org/10.1016/j.agrformet.2007.05.011.

Landsberg, J.J., 1986. Physiological Ecology of Forest Production. Academic Press, New York, NY, USA.

Law, B.E., Waring, R.H., 1994. Combining remote sensing and climatic data to estimate net primary production across Oregon. Ecol. Appl. 4 (4), 717–728.

Lee, C.M., Cable, M.L., Hook, S.J., Green, R.O., Ustin, S.L., Mandl, D.J., Middleton, E.M., 2015. An introduction to the NASA Hyperspectral InfraRed Imager (HyspIRI) mission and preparatory activities, Special Issue on HyspIRI. Remote Sens. Environ. 167:6–19. http://dx.doi.org/10.1016/j.rse.2015.06.012.

Lyapustin, A., Martonchik, J., Wang, Y., Laszlo, I., Korkin, S., 2011. Multi-angle implementation of atmospheric correction (MAIAC): 1. Radiative transfer basis and look-up tables. J. Geophys. Res.-Atmos. 116. http://dx.doi.org/10.1029/2010jd014985 (2011).

Magney, T.S., Vierling, L.A., Eitel, J.U.H., Huggins, D.R., Garrity, S.R., 2016. Response of high frequency Photochemical Reflectance Index (PRI) measurements to environmental conditions in wheat. Remote Sens. Environ. 173, 84–97.

Margolis, H.A., Flanagan, L.B., Amiro, B.D., 2006. The Fluxnet-Canada Research Network: influence of climate and disturbance on carbon cycling in forests and peatlands. Agric. For. Meteorol. 140 (1–4), 1–5.

McCaughey, J.H., Pejam, M.R., Arain, M.A., Cameron, D.A., 2006. Carbon dioxide and energy fluxes from a boreal mixed wood forest ecosystem in Ontario, Canada. Agric. For. Meteorol. 140, 79–96.

Michalak, A.M., Jackson, R.B., Marland, G., Sabine, C.L., et al., 2011. A U.S. carbon cycle science plan. U.S. Global Change Research Program Report. PMEL number 3731.

Middleton, E.M., Sullivan, J.H., Bovard, B.D., DeLuca, A.J., Chan, S.S., Cannon, T.A., 1997. Seasonal variability in foliar characteristics and physiology for boreal forest species at the five Saskatchewan tower sites during the 1994 Boreal Ecosystem-Atmosphere Study (BOREAS). J. Geophys. Res. 102 (D24), 28,831–228844.

Middleton, E.M., Drolet, G., Huemmrich, K.F., Hall, F.G., Knox, R.G., Black, A., Barr, A., Lyapustin, A.I., Gervin, J.C., Margolis, H., 2004. Direct satellite inference of ecosystem light use efficiency for carbon exchange using MODIS on Terra and Aqua. Proceedings, International Geoscience and Remote Sensing Symposium, IGARSS 2004, September 19–24, Anchorage, AK, p. 4.

Middleton, E.M., Cheng, Y.-B., Hilker, T., Black, T.A., Krishnan, P., Coops, N.C., Huemmrich, K.F., 2009a. Linking foliage spectral responses to canopy level ecosystem photosynthetic light use efficiency at a Douglas-fir forest in Canada. Can. J. Remote. Sens. 35 (2), 166–188.

Middleton, E.M., Cheng, Y.-B., Corp, L.A., Huemmrich, K.F., Campbell, P.K.E., Zhang, Q.-Y., Kustas, W.P., Russ, A.L., 2009b. Diurnal and seasonal dynamics of canopy-level solar-induced chlorophyll fluorescence and spectral reflectance indices in a cornfield. Proceedings, 6th EARSeL SIG Workshop on Imaging Spectroscopy, CD-ROM, 12 pp., Tel-Aviv, Israel March 16–19, 2009.

Middleton, E.M., Huemmrich, K.F., Cheng, Y.-B., Margolis, H.A., 2012. Spectral bioindicators of photosynthetic efficiency and vegetation stress. In: Thenkabail, P.S., Lyon, J.G., Huete, A. (Eds.), Hyperspectral Remote Sensing of Vegetation. Taylor & Francis (Cat. # K12019).

Middleton, E.M., Cheng, Y.-B., Campbell, P.E., Huemmrich, K.F., Zhang, Q., Landis, D.R., Kustas, W.P., Daughtry, C.S.T., Russ, A.L., 2014. Directional hyperspectral observations to detect plant stress with the PRI and SIF in a cornfield. Proceedings, 4th Recent Advances in Quantitative Remote Sensing (RAQRS'IV), 9 pp., September 22–26, 2014, Valencia, Spain.

Middleton, E.M., Cheng, Y.-B., Campbell, P.E., Huemmrich, K.F., Corp, L.A., Bernardes, S., Zhang, Q., Landis, D.R., Kustas, W.P., Daughtry, C.S.T., Russ, A.L., 2015. Multi-angle hyperspectral observations with SIF and PRI to detect plant stress & GPP in a cornfield. Proceedings, 9th EARSeL SIG Workshop on Imaging Spectroscopy, CD-ROM, Luxembourg City, Luxembourg, April 2015, p. 10.

Monteith, J.L., 1977. Climate and efficiency of crop production. Philos. Trans. R. Soc. Lond. B 281, 277–294.

Morgenstern, K., Black, T.A., Humphreys, E.R., Griffis, T.J., Drewitt, G.B., Cai, T.B., Nesic, Z., Spittlehouse, D.L., Livingstone, N.J., 2004. Sensitivity and uncertainty of the carbon balance of a Pacific Northwest Douglas-fir forest during an El Nino La Nina cycle. Agric. For. Meteorol. 123, 201–219.

Müller, P., Li, X.P., Niyogi, K.K., 2001. Non-photochemical quenching. A response to excess light energy. Plant Physiol. 125 (4), 1558–1566.

Nakaji, T., Kosugi, Y., Takanashi, S., Niiyama, K., Noguchi, S., Tani, M., Oguma, H., Nik, A.R., Kassim, A.R., 2016. Estimation of light-use efficiency through a combinational use of the photochemical reflectance index and vapor pressure deficit in an evergreen tropical rainforest at Pasoh, Peninsular Malaysia. Remote Sens. Environ. 150, 82–92.

Nichol, C.J., Huemmrich, K.F., Black, T.A., Jarvis, P.J., Walthall, C.L., Grace, J., Hall, F.G., 2000. Remote sensing of photosynthetic light-use efficiency of boreal forest. Agric. For. Meteorol. 101, 131–142.

Peñuelas, J., Baret, F., Filella, I., 1994. Semi empirical-indices to assess carotenoids/chlorophyll ratio from leaf spectral reflectance. Measures physiques et signatures en teledetection. Actes: 341–348. 6th Symposium International de l'ISPRS, Val d'Isere, FRA (1994-01-17–1994-01-21), Toulouse, FRA: CNES.

Peñuelas, J., Filella, I., Gamon, J.A., 1995. Assessment of photosynthetic radiation-use efficiency with spectral reflectance. New Phytol. 131, 291–296.

Peñuelas, J., Garbulsky, M.F., Filella, I., 2011. Photochemical reflectance index (PRI) and remote sensing of plant CO_2 uptake. New Phytol. 191, 596–599.

Potter, C.S., Randerson, J.T., Field, C.B., Matson, P.A., Vitousek, P.M., Mooney, H.A., Klooster, S.A., 1993. Terrestrial ecosystem production – a process model-based on global satellite and surface data. Glob. Biogeochem. Cycles 7 (4), 811–841.

Prince, S.D., 1991. A model of regional primary production for use with coarse-resolution satellite data. Int. J. Remote Sens. 12 (6), 1313–1330.

Prince, S.D., Goward, S.N., 1995. Global primary production: A remote sensing approach. J. Biogeogr. 22 (4–5), 815–835.

Raddi, S., Magnani, F., Pippi, I., 2001. Estimation of light use efficiency for the prediction of forest productivity from remote sensing. Proc. 1st SPECTRA Workshop, ESA SP-474,ESTEC, Noordwijk, The Netherlands.

Raddi, S., Cortes, S., Vicinelli, E., Magnani, F., 2006. Remote sensing of photosynthetic processes by Photochemical Reflectance Index (PRI). Earth Observation for Vegetation Monitoring and Water Management, AIP Conference Preceedings. 852, pp. 227–233.

Rahman, A.F., Gamon, J.A., Fuentes, D.A., Roberts, D., Prentiss, D., 2001. Modeling spatially distributed ecosystem flux of boreal forest using hyperspectral indices from AVIRIS imagery. J. Geophys. Res. 106 (D24), 33,579–33,591.

Rahman, A.F., Cordova, V.D., Gamon, J.A., Schmid, H.P., Sims, D.A., 2004. Potential of MODIS ocean bands for estimating CO2 flux from terrestrial vegetation: a novel approach. Geophys. Res. Lett. 31, L10503. http://dx.doi.org/10.1029/2004GL019778.

Running, S., Nemani, R.R., Heinsch, F.A., Zhao, M., Reeves, M., Hashimoto, H., 2004. A continuous satellite-derived measure of global terrestrial primary production. Bioscience 54 (6), 547–560.

Runyon, J., Waring, R.H., Goward, S.N., Wells, J.M., 1994. Environmental limits on net primary production and light-use efficiency across the Oregon Transect. Ecol. Appl. 4 (2), 226–237.

Russell, G., Jarvis, P.G., Monteith, J.L., 1989. Absorption of radiation by canopies and stand growth. Plant Canopies. In: Russell, G., Marshall, B., Jarvis, P.G. (Eds.), Their Growth, Form and Function. Cambridge University Press, Cambridge, pp. 21–40.

Schaaf, C., Gao, F., Strahler, A., Lucht, W., Li, X., Tsang, T., Strugnell, N., Zhang, X., Jin, Y., Muller, J.-P., Lewis, P., Barmsley, M., Hobson, P., Disney, M., Roberts, G., Dunderdale, M., D'Entremont, R., Hu, B., Liang, S., Privette, J., Roy, D., 2002. First operational BRDF, albedo nadir reflectance products from MODIS. Remote Sens. Environ. 83, 135–148.

Schickling, A., Matveeva, M., Damm, A., Schween, J.H., Wahner, A., Graf, A., Crewell, S., Rascher, U., 2016. Combining sun-induced chlorophyll fluorescence and Photochemical Reflectance Index improves diurnal modeling of gross primary productivity. Remote Sens. 8 (574), 18.

Sims, D.A., Rahman, A.F., Vermote, E.F., Jiang, Z., 2011. Seasonal and inter-annual variation in view angle effects on MODIS vegetation indices at three forest sites. Remote Sens. Environ. 115 (12), 3112–3120.

Soudani, K., Hmimina, G., Dufrêne, E., Berveiller, D., Delpierre, N., Ourcival, J.-M., Rambal, S., Joffre, R., 2014. Relationships between photochemical reflectance index and light-use efficiency in deciduous and evergreen broadleaf forests. Remote Sens. Environ. 144, 73–84.

Stagakis, S., Markos, N., Sykioti, O., Kyparissis, A., 2014. Tracking seasonal changes of leaf and canopy light use efficiency in a *Phlomis fruticosa* Mediterranean ecosystem using field measurements and multi-angular satellite hyperspectral imagery. ISPRS J. Photogramm. Remote Sens. 97:138–151. http://dx.doi.org/10.1016/j.isprsjprs.2014.08.012.

Strachan, I.B., Pattey, E., Salustro, C., Miller, J.R., 2008. Use of hyperspectral remote sensing to estimate the gross photosynthesis of agricultural fields. Can. J. Remote. Sens. 34 (3), 333–341.

Stylinski, C.D., Gamon, J.A., Oechel, W.C., 2002. Seasonal patterns of reflectance indices, carotenoid pigments and photosynthesis of evergreen chaparral species. Oecologia 131, 366–374.

Sun, J., Peng, C., McCaughey, H., Zhou, X., Thomas, V., Berninger, F., St-Onge, B., Hua, D., 2008. Simulating carbon exchange of Canadian boreal forests II. Comparing the carbon budgets of a boreal mixed wood stand to a black spruce forest stand. Ecol. Model. 219, 276–286.

Thornton, P.E., Running, S.W., Hunt, E.R., 2005. Biome-BGC: terrestrial ecosystem process model. Version 4.1.1. Oak Ridge Natl. Lab. Distrib. Act. Arch. Cent. Oak Ridge, Tenn. http://dx.doi.org/10.3334/ORNLDAAC/805 (Available at http://daac.ornl.gov)

Turner, D.P., Urbanski, S., Bremer, D., Wodsy, S.C., Meyers, T., Gower, S.T., Gregory, M., 2003. A cross-biome comparison of daily light use efficiency for gross primary production. Glob. Chang. Biol. 9, 383–395.

van Leeuwen, W., Huete, A.R., Laing, T.W., 1999. MODIS vegetation index compositing approach: a prototype with AVHRR data. Remote Sens. Environ. 69, 264–280.

Vermote, E.F., Tanre, D., Deuzé, J.L., Herman, M., Morcrette, J.J., 1997. Second simulation of the satellite signal in the solar spectrum, 6S: an overview. IEEE Trans. Geosci. Remote Sens. 35, 675–686.

Weng, E., Luo, Y., 2008. Soil hydrological properties regulate grassland ecosystem responses to multifactor global change: a modeling analysis. J. Geophys. Res. 113, G03003. http://dx.doi.org/10.1029/2007JG000539.

Wong, C., Gamon, J.A., 2015a. Three causes of variation in the photochemical reflectance index (PRI) in evergreen conifers. New Phytol. 206:187–195. http://dx.doi.org/10.1111/nph.13159.

Wong, C., Gamon, J.A., 2015b. The photochemical reflectance index provides an optical indicator of spring photosynthetic activation in evergreen conifers. New Phytol. 206: 196–208. http://dx.doi.org/10.1111/nph.13251.

Yuan, W., Liu, S., Zhou, G., Zhou, G., Tieszen, L.L., Baldocchi, D., Bernhofer, C., Gholz, H., Hollinger, D.Y., Hu, Y., Law, B.E., Stoy, P.C., Vesala, T., 2007. Deriving a light use efficiency model from eddy covariance flux data for predicting daily gross primary production across biomes. Agric. For. Meteorol. 143, 189–207.

Yuan, W., Cai, W., Xia, J., Chen, J., Liu, S., Dong, W., Merbold, L., Law, B., Arain, A., Beringer, J., Bernhofer, C., Black, A., Blanken, P.D., Cescatti, A., Chen, Y., Francois, L., Gianelle, D., Janssens, I.A., Jung, M., Kato, T., Kiely, G., Liu, D., Marcolla, B., Montagnani, L., Raschi, A., Roupsard, O., Varlagin, A., Wohlfahrt, G., 2014. Global comparison of light use efficiency models for simulating terrestrial vegetation gross primary production based on the LaThuile database. Agric. For. Meteorol. 192–193, 108–120.

Zarco-Tejada, P.J., González-Dugo, V., Berni, J.A., 2012. Fluorescence, temperature and narrow-band indices acquired from a UAV platform for water stress detection using a micro-hyperspectral imager and a thermal camera. Remote Sens. Environ. 117, 322–337.

Zarco-Tejada, P.J., González-Dugo, V., Williams, L.E., Suárez, L., Berni, J.A., Goldhamer, D., Fereres, E., 2013a. A PRI-based water stress index combining structural and chlorophyll effects: Assessment using diurnal narrow-band airborne imagery and the CWSI thermal index. Remote Sens. Environ. 138, 38–50.

Zarco-Tejada, P.J., Morales, A., Testi, L., Villalobos, F.J., 2013b. Spatio-temporal patterns of chlorophyll fluorescence and physiological and structural indices acquired from hyperspectral imagery as compared with carbon fluxes measured with eddy covariance. Remote Sens. Environ. 133, 102–115.

Zhang, Q.-Y., Middleton, E.M., Margolis, H.A., Drolet, G.G., Barr, A.A., Black, T.A., 2009. Can a MODIS-derived estimate of the fraction of PAR absorbed by chlorophyll ($FAPAR_{chl}$) improve predictions of light-use efficiency and ecosystem photosynthesis for a boreal aspen forest? Remote Sens. Environ. 113, 880–888.

Zhang, Q., Middleton, E.M., Cheng, Y.-B., Huemmrich, K.F., Cook, B.D., Corp, L.A., Kustas, W.P., Russ, A.L., Prueger, J.H., Yao, T., 2016. Integrating fAPARchl and PRInadir from EO-1/Hyperion to predict cornfield daily gross primary production (GPP). Remote Sens. Environ. (submitted 1/2016).